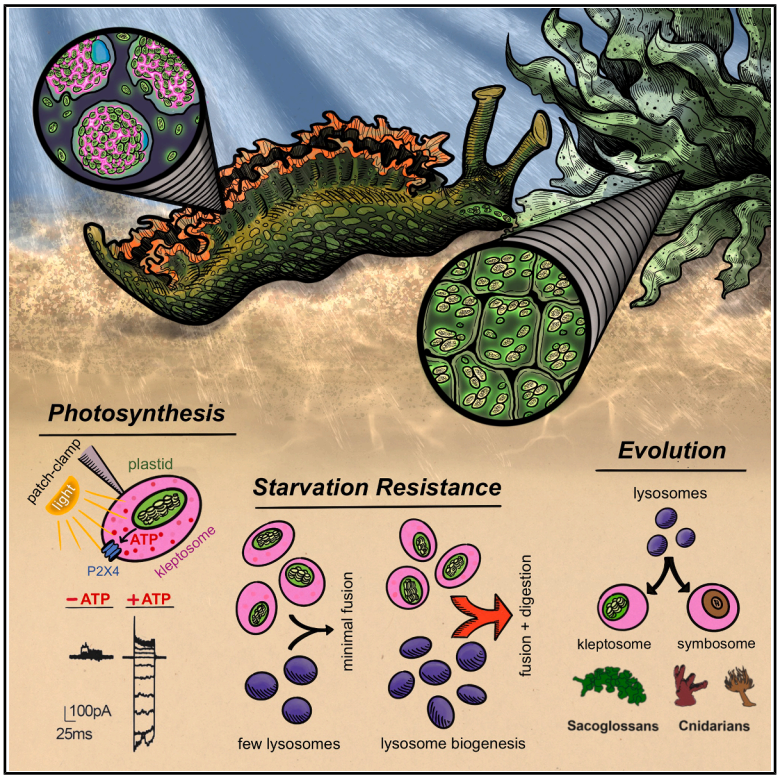
Cell



# A host organelle integrates stolen chloroplasts for animal photosynthesis

## Graphical abstract




## Authors

Corey A.H. Allard, Angus B. Thies, Rishav Mitra, ..., Martin Tresguerres, Amy S.Y. Lee, Nicholas W. Bellono

## Correspondence

corey_allard@hms.harvard.edu (C.A.H. A.), amysy_lee@dfci.harvard.edu (A.S.Y.L.), nbellono@harvard.edu (N.W.B.)

## In brief

Sea slugs steal foreign chloroplasts and store them in specialized organelles that facilitate photosynthesis and eventual digestion to mediate starvation resistance.

## Highlights

- Sea slugs retain and store foreign chloroplasts in kleptosome organelles
- Kleptosomes use luminal ATP-sensing ion channels to support photosynthesis
- Kleptosomes digest chloroplasts during prolonged starvation
- Slugs and corals use convergent mechanisms of endosymbiosis

Allard et al., 2025, Cell *188*, 1–12
September 18, 2025 © 2025 Elsevier Inc. All rights are reserved, including those for text and data mining, AI training, and similar technologies.
https://doi.org/10.1016/j.cell.2025.06.003

CellPress

Please cite this article in press as: Allard et al., A host organelle integrates stolen chloroplasts for animal photosynthesis, Cell (2025), https://doi.org/10.1016/j.cell.2025.06.003

Cell

CellPress

Article

# A host organelle integrates stolen chloroplasts for animal photosynthesis

Corey A.H. Allard,[1,3,6,*] Angus B. Thies,[2] Rishav Mitra,[1] Patric M. Vaelli,[1] Olivia D. Leto,[1,3] Brittany L. Walsh,[1] Elise M.J. Laetz,[4] Martin Tresguerres,[2] Amy S.Y. Lee,[3,5,*] and Nicholas W. Bellono[1,*]

[1]Department of Molecular and Cellular Biology, Harvard University, Cambridge, MA 02138, USA
[2]Marine Biology Research Division, Scripps Institution of Oceanography, University of California, San Diego, La Jolla, CA 92093, USA
[3]Department of Cell Biology, Harvard Medical School, Boston, MA 02115, USA
[4]Groningen Institute for Evolutionary Life Sciences, University of Groningen, Groningen, the Netherlands
[5]Department of Cancer Immunology and Virology, Dana-Farber Cancer Institute, Boston, MA 02115, USA
[6]Lead contact
*Correspondence: corey_allard@hms.harvard.edu (C.A.H.A.), amysy_lee@dfci.harvard.edu (A.S.Y.L.), nbellono@harvard.edu (N.W.B.)
https://doi.org/10.1016/j.cell.2025.06.003

## SUMMARY

Eukaryotic life evolved over a billion years ago when ancient cells engulfed and integrated prokaryotes to become modern mitochondria and chloroplasts. Sacoglossan "solar-powered" sea slugs possess the ability to acquire organelles within a single lifetime by selectively retaining consumed chloroplasts that remain photosynthetically active for nearly a year. The mechanism for this "animal photosynthesis" remains unknown. Here, we discovered that foreign chloroplasts are housed within novel, host-derived organelles we term "kleptosomes." Kleptosomes use ATP-sensitive ion channels to maintain a luminal environment that supports chloroplast photosynthesis and longevity. Upon slug starvation, kleptosomes digest stored chloroplasts for additional nutrients, thereby serving as a food source. We leveraged this discovery to find that organellar retention and digestion of photosynthetic cargo has convergently evolved in other photosynthetic animals, including corals and anemones. Thus, our study reveals mechanisms underlying the long-term acquisition and evolutionary incorporation of intracellular symbionts into organelles that support complex cellular function.

## INTRODUCTION

Endosymbiotic events in which one organism is engulfed and housed within the cells of another have resulted in novel biological functions across the tree of life. For example, essential organelles such as mitochondria and chloroplasts were originally free-living cells that were phagocytosed and integrated into a host cell. Establishment and maintenance of endosymbiosis is therefore a major driver of evolutionary novelty, uniting the physiology of unrelated lineages to produce new traits.

Many endosymbioses result from the engulfment of a photosynthetic microorganism, such as the cyanobacterial ancestor of many chloroplasts or dinoflagellates, by corals. "Solar-powered" Sacoglossan sea slugs appear to have established the beginnings of an endosymbiosis via a distinct route: theft of chloroplasts from an established ancient endosymbiosis in chloroplast-containing algae. These slugs feed on marine algae by piercing cell walls with their radula, sucking out the cell contents,[1] and ingesting and sequestering stolen, photosynthetically active chloroplasts into the cells lining their intestinal diverticula[2–6] (Figure 1A). Sequestered chloroplasts (often termed "kleptoplasts[7]") remain active for nearly a year despite lacking access to the algal nucleus to replenish photosynthetic enzymes.[8,9] Therefore, Sacoglossan sea slugs have evolved the remarkable ability to "steal" functional parts from other organisms and incorporate them within their own bodies.

The mechanisms of sequestration, maintenance, and the fitness advantage provided by ingested chloroplasts to slugs remain unclear.[10–14] Isotope tracing studies have demonstrated that fixed carbon is incorporated into slug tissue, perhaps enhancing feeding through acquisition of photosynthetically derived nutrients.[4,10,15,16] Yet, previous studies demonstrate modest effects of photosynthesis on starvation, suggesting that chloroplasts could afford additional advantages.[6,10,11] For example, ingested chloroplasts could provide environmental camouflage, make slugs unpalatable to predators, or serve as a "living larder" by incorporating a stored reserve food source to be accessed during times of scarcity. Indeed, the longevity of ingested chloroplasts appears to be supported by slug-mediated photoprotection mechanisms.[13,17] Therefore, understanding how chloroplasts are stored and used in slug tissues could provide general insight into how novel organelles are integrated into host cell physiology. By exploring the biology of these unusual animals, we made several serendipitous discoveries,


All rights are reserved, including those for text and data mining, AI training, and similar technologies.

Please cite this article in press as: Allard et al., A host organelle integrates stolen chloroplasts for animal photosynthesis, Cell (2025), https://doi.org/10.1016/j.cell.2025.06.003



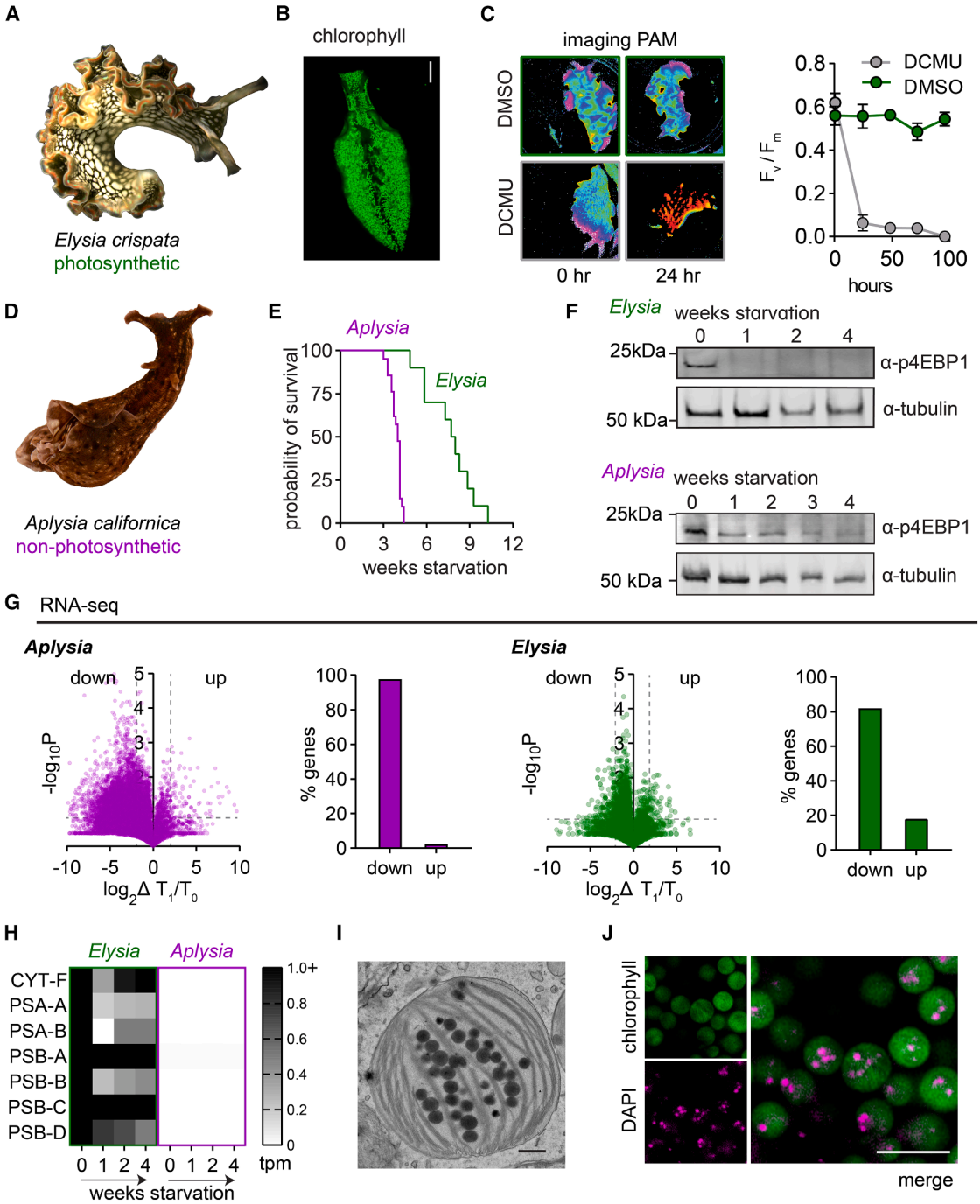



**Figure 1. Photosynthetic slugs maintain transcriptionally active, foreign chloroplasts**

(A) "Photosynthetic" sea slug (*Elysia crispata*).

(B) Autofluorescence of chloroplasts stored within slug tissues. Scale bar, 1 mm.

(C) Pulse amplitude modulated (PAM) fluorometry demonstrated that slugs maintain photosynthetic efficiency that was abolished by the photosynthesis inhibitor DCMU ($n$ = 3 up to 48 h, 1–3 to 96 h).

(D) Non-photosynthetic slug *Aplysia californica*.

(E) Photosynthetic *Elysia crispata* survived longer than non-photosynthetic *Aplysia californica* during starvation (Elysia $n$ = 10, Aplysia $n$ = 21).

(F) mTOR activity (assessed by 4E-BP1 phosphorylation) decreased at a similar rate during starvation of *Elysia* or *Aplysia* slugs. Tubulin was used as a loading control. ($n$ = 3).

*(legend continued on next page)*

Please cite this article in press as: Allard et al., A host organelle integrates stolen chloroplasts for animal photosynthesis, Cell (2025), https://doi.org/10.1016/j.cell.2025.06.003





demonstrating that chloroplasts are stored within unique cells and organelles specialized to promote multiple functions of chloroplasts that depend on the internal state of the animal host.

## RESULTS

### Chloroplasts are stored in specialized kleptosome organelles

Sacoglossan sea slugs exhibit remarkable resistance to starvation.[6,8,10,18,19] How do slugs maintain foreign, functional chloroplasts during starvation without access to the algal nucleus to replenish photosynthetic proteins? Despite longstanding questions regarding horizontal transfer of algal genes to the animal nucleus, it was recently demonstrated slugs do not encode photosynthetic genes.[20] Therefore, we reasoned that slugs could use unique gene regulation programs to support chloroplast function during starvation. To probe this hypothesis, we compared the starvation resistance of the Sacoglossan sea slug *Elysia crispata*, which we confirmed retains functional chloroplasts (Figures 1A–1C), and the non-photosynthetic sea slug *Aplysia californica*, which consumes algae but does not retain functional chloroplasts (Figure 1D). Using similarly sized slugs, all *Aplysia* died after 3–4 weeks of starvation, but *Elysia* survived to nearly 4 months (Figure 1E). We considered that *Elysia* could either be more resistant to starvation or could begin starving more slowly due to nutritional advantages provided by stored chloroplasts. Therefore, we compared the activity of the key metabolic regulator mTOR by probing its substrate 4E-BP1 to reveal that mTOR was inactivated in both *Elysia* and *Aplysia* by 1 week of starvation, suggesting that *Elysia* slugs normally enter starvation (Figures 1F and S1A–S1C). Consistent with this finding, RNA sequencing (RNA-seq) analyses revealed global downregulation of slug transcription after 1 week of food withdrawal in both *Elysia* and *Aplysia* (Figure 1G). The few upregulated genes included those involved in starvation responses, such as a negative regulator of transcription (Ylpm1), a chaperon active during glucose starvation (Hspa5), and an autophagosome assembly factor (Vmp1).[21–23]

Thus, to our surprise, *Elysia* did not exhibit an obvious upregulation in slug-encoded transcriptional programs that might enable chloroplast function during starvation. Instead, we found that expression of chloroplast-encoded transcripts critical for photosynthesis maintained high expression levels in *Elysia* slugs over 4 weeks of starvation but were absent from *Aplysia* at all time points (Figure 1H). Accordingly, *Elysia* chloroplasts contained morphologically intact thylakoid membranes required for photosynthesis and retained nucleoids required for transcription of plastid-encoded genes that contribute to chloroplast function (Figures 1I and 1J). Therefore, we conclude that *Elysia* slugs maintain transcriptionally active and functional chloroplasts but do not exhibit an obvious slug-encoded transcriptional program to support chloroplast function during starvation.

We next asked if *Elysia* slugs instead support imported chloroplasts by providing them with slug proteins that substitute for photosynthetic machinery normally encoded by the algal nucleus. We performed Click chemistry labeling of newly synthesized proteins in live slugs, isolated their chloroplasts, and extracted labeled proteins for proteomic analysis (Figures 2A–2C). Surprisingly, we found that the vast majority of peptides identified in the isolated chloroplast preparations mapped to slug rather than plant or algal proteins, supporting our hypothesis that the slugs provide the chloroplasts with new proteins (Figure 2D; Table S1). We also found that some nascent peptides mapped to algal chloroplast proteins involved in photosynthesis and plastid translation, consistent with our observation that chloroplast gene expression persists in starved slugs (Figures 2E and 2F). While we expected chloroplast-localized slug proteins to be involved with functions that might support photosynthesis, there were no obvious candidates that could serve such functions. Instead, we curiously observed that endocytosis/phagocytosis was among the most enriched Gene Ontology (GO) categories in our proteomic analysis (Figures 2E–2G).

We next wondered if chloroplasts could be stored within slug-derived organelles, thereby explaining why slug endosomal proteins "contaminated" our chloroplast proteomic results. Whereas most large cargoes enter cells through endocytosis, previous electron microscopy analysis of ingested chloroplasts reported contradictory findings regarding the presence of a membrane engulfing chloroplasts.[24–28] To determine whether ingested chloroplasts reside in endosome-like organelles, we searched our proteomic data for molecular markers diagnostic of the endocytic stages. The phagosome marker Rab7a was the most abundant endosomal protein (Figure 2H), suggesting that chloroplasts could be stored in organelles similar to arrested phagosomes. Accordingly, we found that stolen chloroplasts reside within specific individual cells from the slug's digestive tract (we termed plastid cells) that we hypothesize are specialized for housing stolen chloroplasts (Figure 2J). Upon lysing those cells, the membrane marker FM1-43 labeled a clear and distinct membrane around each individual stolen chloroplast (Figures 2K and S2B). Furthermore, the membrane surrounding isolated chloroplasts was robustly positive for traditional markers of phagosomes and phagolysosomes, including the ATP-sensing ion channel P2X4, the vacuolar proton pump VHA, the lipid transporter NPC-2, and Rab7 (Figures 1K and S2A–S2C). There was some heterogeneity in Rab7 signal intensity across individual organelles, which will be discussed later in the study. Thus, we termed these chloroplast-containing organelles kleptosomes and hypothesized that they represent phagosomes specialized

(G) RNA-seq experiments comparing fed slugs to those starved for 1 week show that both *Elysia crispata* and *Aplysia californica* exhibit global downregulation of transcription. $n = 3$ per species per time point).

(H) Expression of chloroplast-encoded photosystem (PS) genes and cytochrome F are maintained in starving *Elysia crispata* but absent in *Aplysia californica*. TPM, transcripts per million. ($n = 3$).

(I) Intact membrane structure of stolen chloroplasts visualized by transmission electron microscopy. Scale bar, 500 nm.

(J) Chloroplast nucleoids remain present in stolen chloroplasts. Scale bar, 5 μm.

See also Figure S1.

Please cite this article in press as: Allard et al., A host organelle integrates stolen chloroplasts for animal photosynthesis, Cell (2025), https://doi.org/10.1016/j.cell.2025.06.003



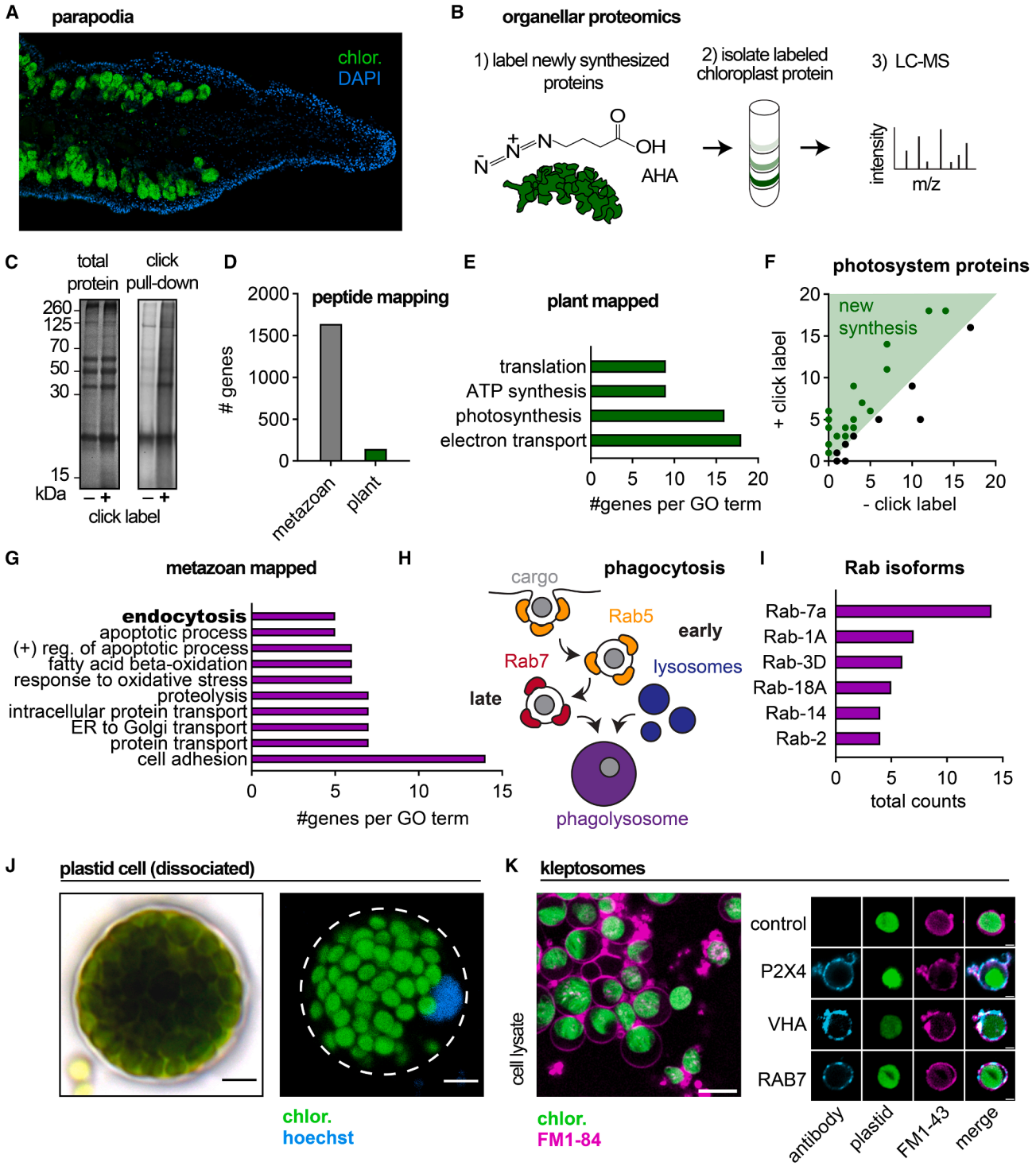



**Figure 2. Photosynthetic slugs store stolen chloroplasts in endosome-like organelles called kleptosomes**

(A) Stolen chloroplasts are stored in the leaf-like parapodia on the back of *Elysia crispata* slugs. Chlor., chlorophyll autofluorescence.

(B) Proteomic analysis pipeline. Newly synthesized proteins in slugs were labeled with L-azidohomoalanine (AHA), chloroplasts were extracted, and AHA-labeled proteins were isolated for liquid chromatography-mass spectrometry (LC-MS).

C) Streptavidin pull-down of click-labeled proteins indicated widespread labeling in chloroplasts extracted from slugs. Coomassie stain of total protein was used to demonstrate specific labeling.

(D) Nearly all newly synthesized peptides extracted from chloroplasts mapped to metazoan (animal) rather than plant or algal genes.

*(legend continued on next page)*

Please cite this article in press as: Allard et al., A host organelle integrates stolen chloroplasts for animal photosynthesis, Cell (2025), https://doi.org/10.1016/j.cell.2025.06.003



for maintaining functional chloroplasts that are arrested at a stage preceding fusion with the lysosome.

## Kleptosomes support chloroplast retention and function

Phagosomes are membrane-bound organelles that compartmentalize their lumen from the surrounding cytosol to establish a distinct physiological space that can be regulated by cellular signals. For example, the phagosome lumen becomes increasingly acidic as organelles transition from early to late endosomes, and this acidic pH activates lysosomal enzymes involved in breaking down and recycling cargos. We reasoned that kleptosomes might similarly regulate the chemistry and physiology of their lumen to support chloroplast longevity and photosynthesis and facilitate communication between foreign chloroplasts and slug cells. Indeed, our proteomic and histological analyses demonstrate that the kleptosomal membrane contains putative ion channels, pumps, and biomolecular transporters consistent with the establishment of a regulated compartment.

To explore whether the kleptosome establishes an intracellular microenvironment that supports chloroplast function, we sought to characterize this novel membrane using direct recordings with whole-organelle patch-clamp electrophysiology. Measurements from isolated kleptosomes revealed minimal basal currents during voltage protocols, demonstrating the presence of an ion-impermeable membrane. Importantly, this is inconsistent with the outer chloroplast membrane that is porous and permeable to small molecules and ions. We then asked whether physiological signals from stored chloroplasts could regulate the kleptosome membrane. In this respect, a major function of chloroplasts is to convert light energy into adenosine triphosphate (ATP), which therefore could be enriched in chloroplast-containing kleptosomes and signal their presence within slug cells. Indeed, consistent with localization of the ATP-sensitive P2X4 receptor to the kleptosome membrane, luminal ATP elicited inwardly rectifying currents that were enhanced by the P2X potentiator ivermectin and blocked by addition of the P2X4 antagonists copper or 5-BDBD (Figures 3A–3D, top row). P2X4 receptors are inhibited by acidic pH and insensitive to the broad P2X antagonists suramin or pyridoxalphosphate-6-azophenyl-2′,4′-disulfonic acid (PPADS). These properties matched the ATP-gated conductance in kleptosomes, suggesting these currents are mediated by P2X4 (Figures S3A and S3B). We then cloned and heterologously expressed *E. crispata* P2X4 (eP2X4), which localized to HEK293 endolysosomes (Figure 3B). This is consistent with native kleptosome localization and that of the well-characterized mammalian P2X4 (rat, rP2X4) (Figure S3C). Furthermore, eP2X4 mediated endolysosomal currents that biophysically and pharmacologically matched both rP2X4 and native kleptosomes. Thus, we conclude that eP2X4 forms the ATP-sensitive ion channel in kleptosomes (Figures 3A–3D, middle and bottom row; Figures S3D and S3E).

We next leveraged the characterization of eP2X4 to ask if the kleptosome membrane supports the storage of photosynthetically active chloroplasts. We found that perturbing P2X4 with the antagonist 5-BDBD significantly decreased net photosynthetic oxygen production by 62% ($p_{adj}$ = 0.0250) (Figure 3E). This effect was similar, albeit less pronounced, to that induced by the photosynthesis-blocking agent DCMU (Figure 3E). Importantly, respiratory oxygen consumption was not affected, indicating that these treatments did not disrupt global slug physiology (Figure 3E). Thus, we conclude that the kleptosome membrane is a regulated signaling hub that supports the photosynthetic function of chloroplasts (Figure 3F).

## Kleptosomes digest chloroplasts during prolonged starvation

How do kleptosomes regulate chloroplasts to promote starvation resistance? We noticed that slugs turned orange after more than 4 weeks of starvation, reminiscent of the leaves of trees during autumn (Figure 4A).[29] Autofluorescence from chlorophyll that is present in fed green slugs was absent from starved orange slugs, indicating chloroplast degradation. Indeed, oxygen production in orange slugs was not affected by the photosynthesis inhibitor DCMU, demonstrating that starved slugs are not photosynthetic (Figure 4B). Accordingly, 6 weeks of starvation led to downregulation of photosystem genes (Figure 4C, log scale). We therefore hypothesized that slugs use chloroplasts for photosynthesis and then "digest" stored chloroplasts during prolonged starvation as a last-resort energy source.

To test this possibility, we first compared the autofluorescence of chloroplasts stored in kleptosomes of cells within distal parapodia to those found in the slug's digestive tract. Whereas kleptosome-stored chloroplasts exhibited bright far-red autofluorescence emission indicative of photosynthetic pigments such as chlorophyll, chloroplasts in the digestive tract lumen were dim. Spectral analyses revealed chloroplasts that were dim in the far-red channel (650–700 nm) were brighter in the green channel (500–550 nm), suggesting a change in pigment properties that could represent the breakdown of chlorophyll and other photosynthetic pigments (Figures 4D and S4A–S4C).

(E) Translational activity of chloroplasts was demonstrated by Gene Ontology (GO) categories of plant-mapped proteins, which featured electron transport, photosynthesis, ATP synthesis, and translation as the most enriched categories.
(F) Photosystem proteins were enriched in click-labeled (green shading) vs. unlabeled (nonspecific) chloroplast samples, further demonstrating maintenance of chloroplast translation in slugs.
(G) Top GO categories of metazoan-mapped proteins included intracellular transport categories, oxidative stress, and endocytosis.
(H) Schematic of phagocytosis illustrating key events leading to lysosomal fusion.
(I) Rab7a was the most abundant Rab protein identified in chloroplasts extracted from slugs.
(J) Stolen chloroplasts accumulate in specific slug "plastid cells." Chlor., chlorophyll autofluorescence. Bright-field (left) and confocal (right) imaging; scale bars, 5 μm.
(K) Isolated chloroplasts from slugs were stained with the lipophilic dye FM-143 (magenta) to reveal a clear membrane surrounding chloroplasts (autofluorescent chlorophyll, green). The membrane stained with antibodies recognizing the late-stage endosomal marker Rab7, proton pump VHA, and endosomal cation channel P2X4, suggesting its phagosomal origin. We named this slug-derived chloroplast storage organelle the kleptosome. Scale bars, 1 μm.
See also Figure S2.

Please cite this article in press as: Allard et al., A host organelle integrates stolen chloroplasts for animal photosynthesis, Cell (2025), https://doi.org/10.1016/j.cell.2025.06.003



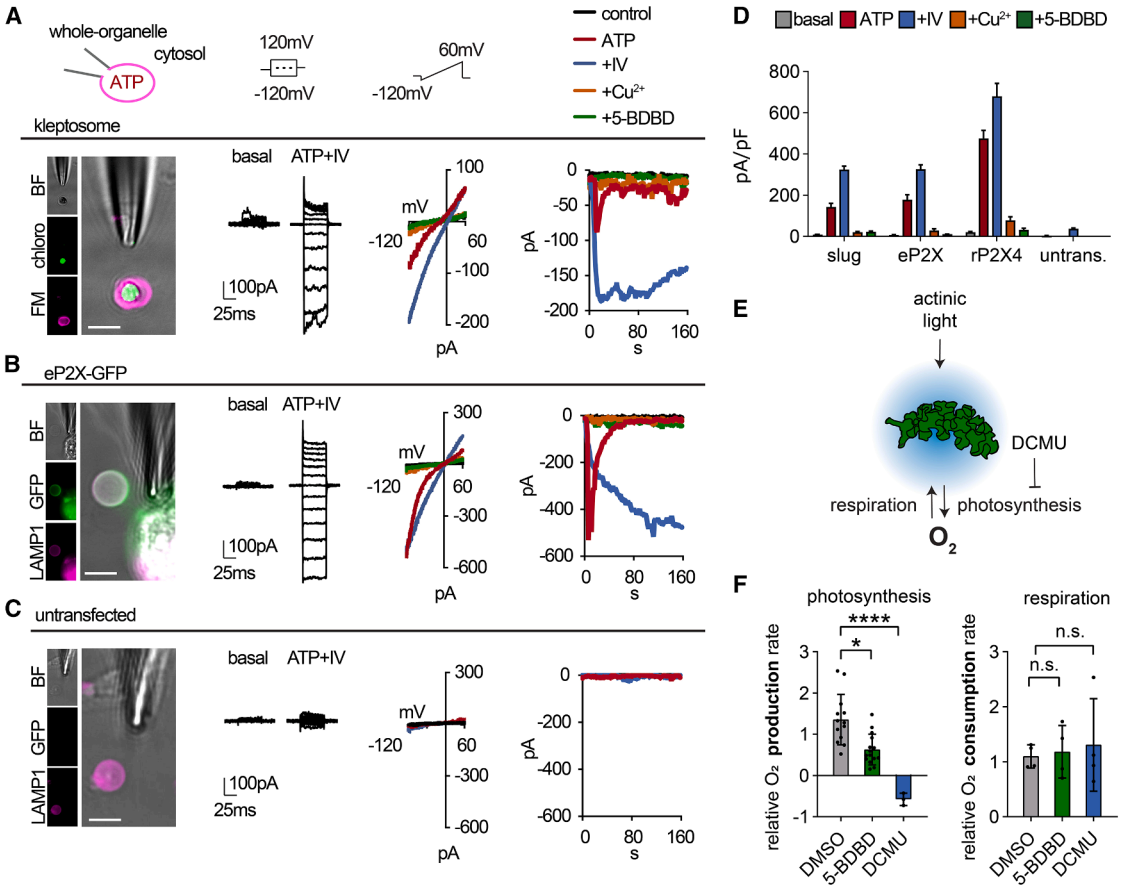



**Figure 3. Kleptosomes transduce luminal signals with ATP-sensitive ion channels to support photosynthesis**

(A) (Left) Patch-clamp preparation for an isolated chloroplast-containing kleptosome stained with live-cell FM dye. (Middle) Large currents were recorded in the presence of 1 mM adenosine triphosphate (ATP) + modulator 5 μM ivermectin (IV) in the lumen during voltage steps. (Right) Whole-organellar currents recorded in response to voltage ramps show that native kleptosomes exhibited ATP-sensitive currents that were enhanced by ivermectin and inhibited by P2X4 blockers 500 μM $Cu^{2+}$ or 100 μM 5-BDBD. Scale bar, 5 μm.

(B) (Left) Heterologously expressed *E. crispata* P2X4 (eP2X4) tagged with GFP localized to enlarged endolysosomes in HEK293 cells. Image shows a lysosome excised from a cell for patch-clamp. (Middle) Patch-clamp recordings demonstrate that eP2X4 was activated by ATP + ivermectin during voltage steps. (Right) Voltage ramp experiments show currents induced by ATP and ivermectin were blocked by $Cu^{2+}$ or 5-BDBD, similar to native kleptosomes. Scale bar, 5 μm.

(C) Endolysosomes from untransfected AD293 cells exhibited much smaller currents in response to ATP + ivermectin in patch-clamp experiments, as in (A) and (B). Scale bars, 5 μm.

(D) The pharmacological profile of native kleptosomes was the same as heterologously expressed eP2X4 or rat P2X4 (rP2X4). Ivermectin increased ATP-elicited currents, while $Cu^{2+}$ or 5-BDBD similarly blocked activity. Peak amplitudes were measured at −120 mV. Two-way ANOVA with post hoc Tukey test ($n$ = 3–5 organelles), $p < 0.05$ for ATP and ivermectin in native kleptomes or endolysosomes expressing eP2X4 or rP2X4. Data are mean ± SEM.

(E) Slugs produce oxygen through photosynthesis and consume consumption through respiration. Each measurement was normalized to an initial measurement lacking drug such that values of 1 signify no change. Relative oxygen consumption or production serves as a proxy for photosynthetic output of stolen chloroplasts.

(F) Photosynthetic oxygen production in 500 μE light was reduced by P2X4 blocker 5-BDBD and the photosynthesis inhibitor DCMU (Welch's ANOVA $p < 0.0001$, Dunnett's T3 multiple comparisons test $p_{adj}$ = 0.017 for 5-BDBD, <0.0001 for DCMU vs. solvent control). Oxygen consumption measured in darkness was unchanged by addition of 5-BDBD or DCMU (Welch's ANOVA test, $p$ = 0.8758).

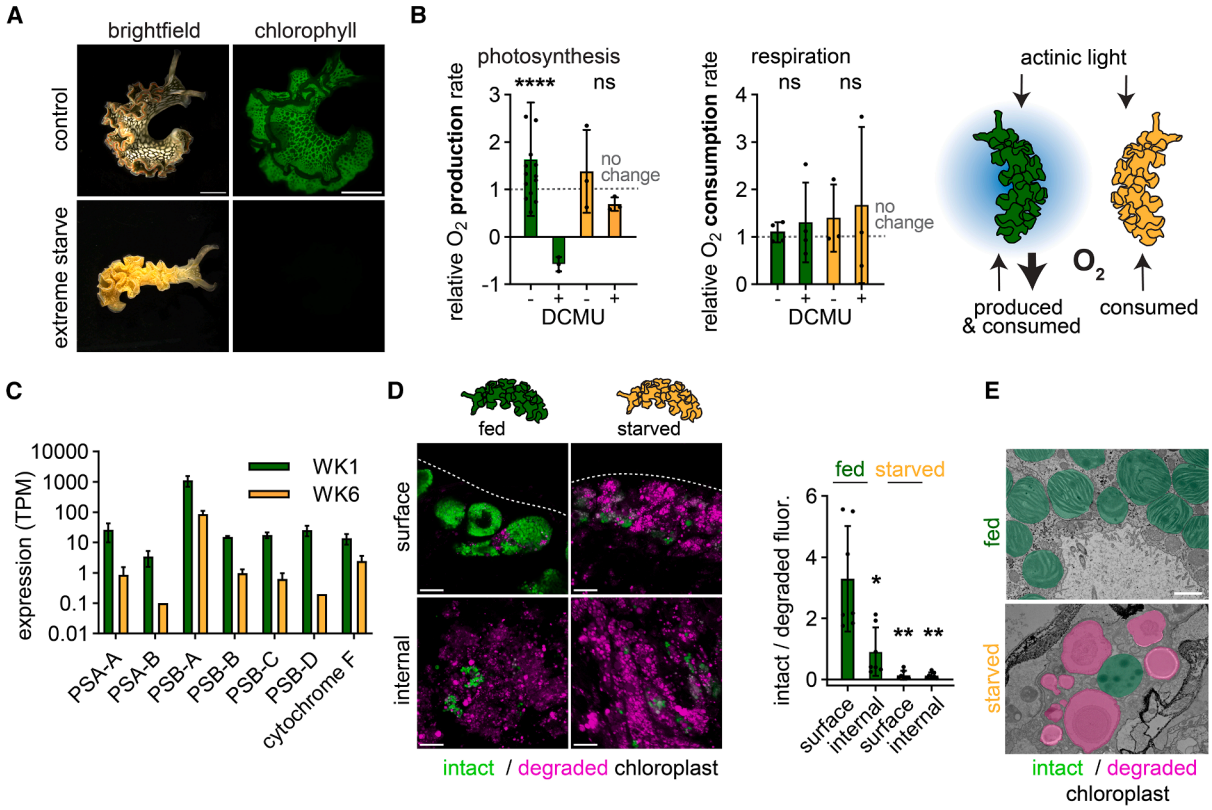
See also Figure S3.

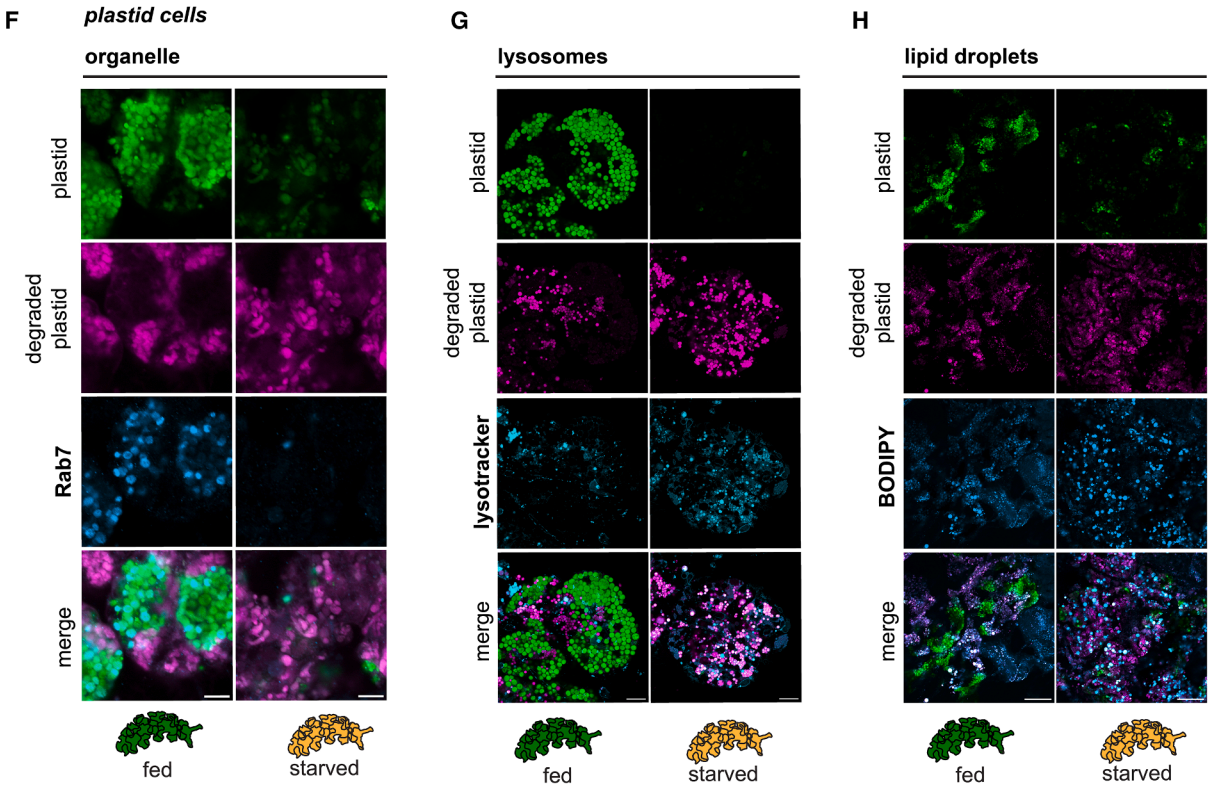
We exploited this observation to image "healthy" and "degraded" chloroplasts in tissues from fed slugs and found that chloroplasts within kleptosomes of cells lining the slug's body surface were overwhelmingly healthy, emitting fluorescence in the far red, whereas the digestive tract lumen was filled with degraded chloroplasts (Figure 4D).[30] Transmission electron microscopy confirmed that chloroplasts within cells had ultrastructure consistent with active photosynthesis, including clear stacks of thylakoid membranes, whereas chloroplasts in the digestive tract contained fewer and poorly defined thylakoids and were often found proximal to structures that resembled lipid droplets (Figure 4E). By contrast, chloroplasts in starved slugs were overwhelmingly degraded throughout the slug (Figure 4D). We conclude that during starvation, chloroplast structure and

Please cite this article in press as: Allard et al., A host organelle integrates stolen chloroplasts for animal photosynthesis, Cell (2025), https://doi.org/10.1016/j.cell.2025.06.003








(legend on next page)

Please cite this article in press as: Allard et al., A host organelle integrates stolen chloroplasts for animal photosynthesis, Cell (2025), https://doi.org/10.1016/j.cell.2025.06.003



functionality break down, and slugs lose photosynthetic activity in their tissues.

Chloroplast degradation during starvation could (1) represent a passive process, reflecting the slug's inability to sustain functional chloroplasts, or (2) be an active process in which chloroplasts are ''digested.'' The latter hypothesis is supported by the observation that extreme starvation switches chloroplasts within cells to resemble those in the digestive tract. We reasoned that chloroplast degradation could be achieved if extreme starvation resulted in a release of the apparent block in the phagocytic pathway that prevents fusion of the kleptosome with lysosomes in fed slugs. We compared localization of the late-stage phagosome marker Rab7 in fed and starved slugs and found that Rab7 was absent from the membranes of organelles containing completely digested chloroplasts (Figures 4E and S4D). Instead, chloroplast-containing cells from starved slugs were enriched for lysosomes (LysoTracker positive) and accumulated lipid droplets (BODIPY positive) (Figures 4G and 4H). These lipid droplets could result from the conversion of chloroplasts into lipids for energy during starvation. But given their abundance in animals near terminal starvation, lipid droplets more likely represent a waste product derived from chloroplast degradation. Indeed, whereas the plastid cells of slugs grown in the presence of food contain very few lysosomes, we observed many more lysosomes in the cells of starved slugs. This suggests that tuning lysosome abundance and availability for fusion could serve as a mechanism regulating kleptosome storage versus digestion (Figure S5). Accordingly, we observed low but detectable rates of chloroplast digestion in fed slugs, suggesting that the few observed lysosomes are capable of fusing with kleptosomes (Figure 4D and S5).

Collectively, these data support a model in which slugs use specialized kleptosome organelles to retain and maintain functional chloroplasts for photosynthetic nutrients. Then, during prolonged starvation (>6 weeks), slugs switch from retention to digesting stored chloroplasts for an additional ''last-resort'' energy source. We propose that kleptosomes represent specialized phagosome-like organelles that function to support photosynthesis in animal cells as well as control, and often delay, flux of stolen chloroplasts through the endocytic system. While the molecular mechanism that governs the switch from retention to degradation is unclear, our data indicate that fed slugs have a limited pool of lysosomes, thereby preventing kleptosome fusion and preserving chloroplast function and ultrastructure. We infer that prolonged starvation stimulates lysosome biogenesis and subsequent fusion with kleptosomes for degradation. Thus, regulation of lysosome biogenesis and associated phagosome arrest could represent a broad adaptation for incorporating foreign organelles that could be tuned through the modulation of signaling pathways at the organellar membrane.

## Convergent evolution of photosynthetic endosymbionts

Kleptosomes in Sacoglossan slugs are reminiscent of the storage organelles that corals and other cnidarians have evolved to store endosymbiotic algae.[31,32] While slugs ingest and functionally retain only chloroplasts from their diet, corals form long-term associations with entire unicellular algae from their environment. Endosymbiotic algae maintain their own chloroplasts as normal, thereby supporting photosynthesis within their cnidarian hosts. Mounting evidence suggests that corals can regulate the abundance of their symbionts by digesting or expelling them.[33–38] Therefore, the storage of functional, photosynthetic cargoes within arrested organelles has convergently evolved in sea slug mollusks and cnidarians, including corals and anemones (Figure 5A). Considering cnidarian organelles also contain phagosomal markers,[39] we wondered whether these divergent lineages might have convergently evolved similar storage organelles for their distinct photosynthetic cargoes. To relate cargo function to phagocytic environment, we probed the localization of kleptosomal proteins in the organelles that store endosymbionts in the soft coral *Lobophytum sp.* and the sea anemone *Exaiptasia diaphana* (Figure 5A). Rab7 is a conserved marker of late-stage phagosomes and phagolysosomes but is absent in early endosomes and after phagosomes fuse with lysosomes to degrade luminal contents. Indeed, we noticed the presence of Rab7 on some but not all kleptosomes in our initial

**Figure 4. Stolen chloroplasts are digested during extreme starvation**

(A) Slugs starved for extreme duration (>6 weeks) turned orange and lost chlorophyll autofluorescence. Scale bar, 5 mm.

(B) DCMU treatment affected the rate of photosynthetic oxygen production rates in 500 μE light for green but not orange slugs, indicating an absence of photosynthesis in orange slugs. Unpaired t test with Welch's correction, $p = 0.3042$. Oxygen consumption measured in darkness was unchanged by addition of DCMU, further demonstrating the absence of photosynthesis (unpaired t test with Welch's correction, $p = 0.8096$).

(C) Time series RNA-seq showed that expression of some photosystem genes decreased after 6 weeks of starvation (orange) compared with fed slugs (green), indicating eventual loss of active chloroplasts. TPM, transcripts per million (logarithmic scale). $n = 3$ slugs per time point. Data were plotted on log scale given wide variation in expression levels among photosystem genes. t test with Welch's correction. PSA-A, $p = 0.259$ (n.s.); PSA-B, $p = 0.214$ (n.s.); PSB-A, $p = 0.1334$ (n.s.); PSB-B, $p = 0.003$ (**); PSB-C, $p = 0.0445$, PSB-D; $p = 0.1229$ (n.s.); cytochrome F, $p = 0.1573$ (n.s.).

(D) Green coloration indicates far-red emission from healthy chloroplasts in plastid cells of fed slugs, while magenta indicates shorter wavelength emission from degraded chloroplasts in the digestive diverticula or throughout in starved slugs. Scale bars, 25 μm, $p_{adj} = 0.029$ fed surface vs. internal, 0.008 fed surface vs. starved surface, 0.008 fed surface vs. starved surface, ANOVA with Dunnett's multiple comparison test).

(E) Transmission electron microscopy showed morphologically intact chloroplasts (green) in fed slugs, while starved slugs contained lipid-droplet-like organelles (magenta). Scale bar, 2 μm.

(F) Kleptosomes in fed vs. extremely starved slugs. Rab7 (cyan) labeled kleptosomes surrounding healthy chloroplasts (far-red autofluorescence in green) but not digested chloroplasts (green autofluorescence, in magenta). Scale bar, 10 μm.

(G) Lysosome distribution in fed vs. extremely starved slugs. LysoTracker (cyan) co-labeled with organelles surrounding digested chloroplasts (green autofluorescence, in magenta) but not healthy chloroplasts (far-red autofluorescence, in green). Scale bar, 10 μm.

(H) Lipid droplet distribution in fed vs. extremely starved slugs. BODIPY (cyan) co-labeled with organelles surrounding digested chloroplasts (green autofluorescence, in magenta) but not healthy chloroplasts (far-red autofluorescence, in green). Scale bar, 50 μm.

See also Figures S4 and S5.

Please cite this article in press as: Allard et al., A host organelle integrates stolen chloroplasts for animal photosynthesis, Cell (2025), https://doi.org/10.1016/j.cell.2025.06.003





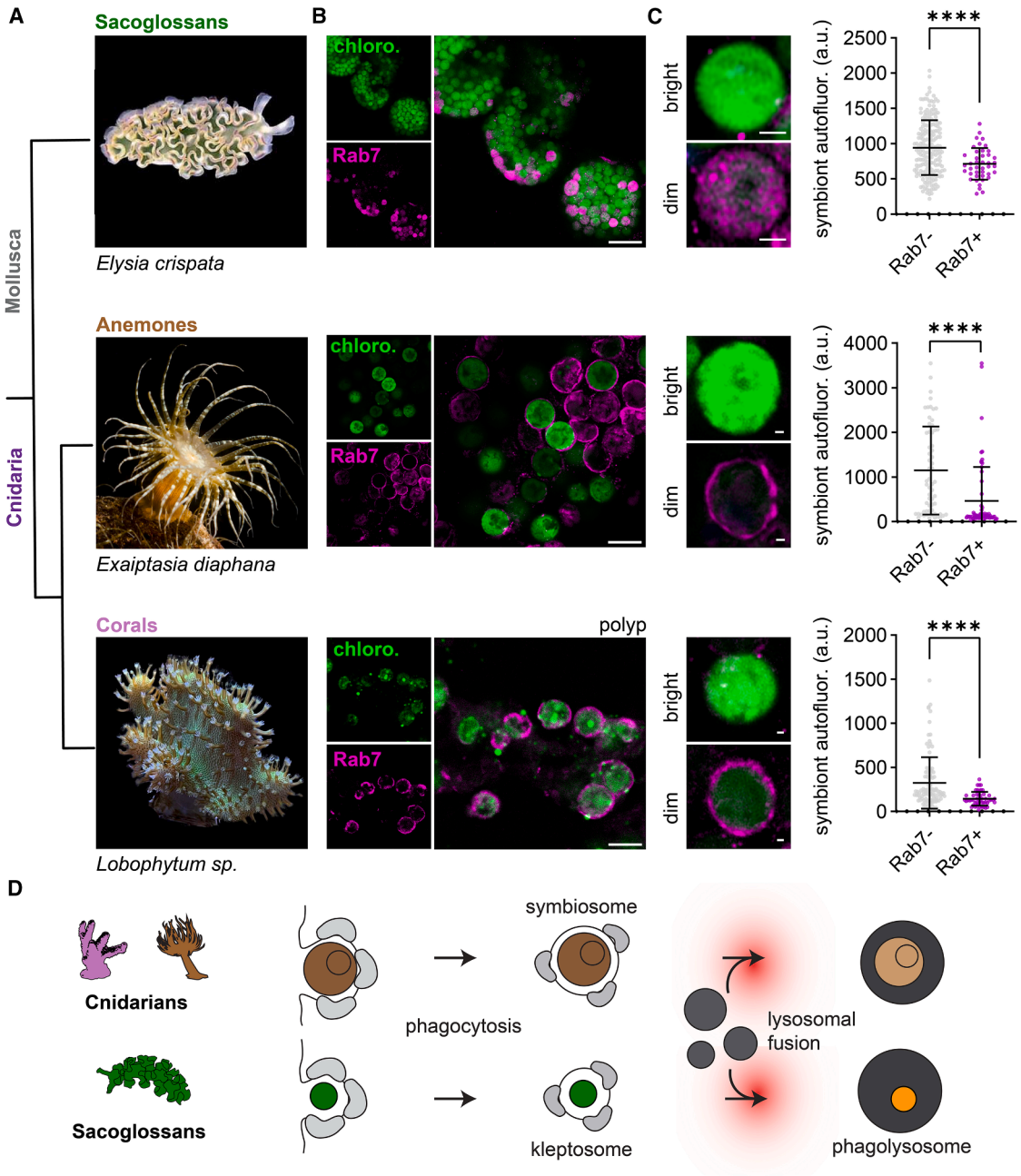



**Figure 5. Convergent evolution of photosynthetic endosymbionts in slugs and corals**

(A) Cladogram of Sacoglossan slugs (mollusk), sea anemones (cnidarian), and corals (cnidarian).

(B) Marker of late-stage endosomes Rab7 localizes to slug kleptosomes and symbiosomes from corals and anemones. Chlorophyll autofluorescence in green, Rab7 immunolabeling in magenta. Scale bar, 10 μm.

(C) Rab7 is enriched on kleptosomes and symbiosomes containing dim vs. bright chloroplasts. Chlorophyll autofluorescence in green, Rab7 immunolabeling in magenta, $p < 0.0001$ for all three species, t test with Welch's correction. Scale bar, 1 μm.

(D) Model of convergent arrest mechanism by modulation of lysosome biogenesis in endosymbiotic mollusks and cnidarians. See text for details.

imaging of slug cells. We therefore compared the intensity of Rab7 immunolabeling to chlorophyll autofluorescence in individual organelles from both slugs and cnidarians as an indicator of chloroplast function vs. phagocytic stage (Figures 5B–5D). In cells of all three animals, we found that the brightest, healthy symbionts or chloroplasts were surrounded by relatively little Rab7, which was instead enriched on organelles containing dimmer, partially degraded symbionts or chloroplasts. Therefore, both slugs and cnidarians store photosynthetic cargo in specialized phagosomes that arrest early in maturation, before

Please cite this article in press as: Allard et al., A host organelle integrates stolen chloroplasts for animal photosynthesis, Cell (2025), https://doi.org/10.1016/j.cell.2025.06.003



accumulation of late-stage phagocytic marker Rab7 and eventual fusion with lysosomes for digestion.

We conclude that storage of photosynthetic cargos in molluscan and cnidarian organelles depends on convergent cellular mechanisms that prevent lysosomal fusion in each lineage. In both phyla, host signaling pathways converge on context-dependent regulation of phagocytic arrest and lysosome biogenesis to determine endosymbiont fate. For example, corals are known to expel their algal symbionts during exposure to environmental stressors that trigger bleaching events, and we find that slugs digest chloroplasts during prolonged starvation.[40] Delineation of the molecular pathways and their specialization across diverse lineages will therefore play a critical role in understanding how foreign organelles and cells integrate into the physiology of their host. Our study provides a framework by which to examine the molecular and cellular mechanisms of establishing endosymbiosis and the eventual evolutionary transition to novel integrated organelles in diverse organismal contexts.

## Limitations of the study

A major limitation is that there are almost no experimental tools or protocols in *Elysia*—a wild-caught animal that is often difficult to source—thereby limiting our ability to manipulate and measure at the scale one would typically use to probe organellar physiology and function. Following our initial discovery and characterization of the kleptosome, future proteomic and microscopy approaches could be developed to ask additional questions about chloroplast function, inter-organellar contacts and signaling, organellar biogenesis, state-dependent shifts in chloroplast and slug transcription and translation, and relationships to other endosymbiotic systems.

In this respect, while our results suggest that kleptosomes represent a major contributor to chloroplast maintenance and longevity, foreign chloroplasts are still missing major components from the algal nuclear genome. Stolen chloroplasts may overcome this limitation by transcribing and translating a majority of their photosynthetic proteins, as algal chloroplasts internally encode a greater percentage of machinery vs. those from plants.[41] This molecular organization allows algal chloroplasts to exist in isolation for longer periods, likely enhanced by slug-mediated photoprotection mechanisms.[13,17]

Similarly, details concerning how kleptosomal P2X4 relates to specific chloroplast functions remain unclear and represent an interesting future direction when technical advances allow (genetics, biosensors, etc.). In the case of corals, an acidic symbiosomal lumen facilitates protons reacting with bicarbonate to produce a local pool of $CO_2$ in the organellar lumen to serve as a substrate for photosynthesis.[31,32] One possibility is that kleptosomal P2X4 senses chloroplast presence via photosynthetic ATP production and conducts cations out of the kleptosome lumen while positively charged protons are pumped into the lumen by V-ATPase proton pumps such as VHA—thus acting as an electrical shunt for ATPase activity. Similarly, mammalian lysosomal cation channels are thought to facilitate an electrical shunt for V-ATPase proton pump activity that establishes an acidic pH favorable for enzymatic activity. Yet, the mechanism of this ionic homeostasis across the endosomal pathway has been challenging to study due to technical challenges associated with organellar patch-clamp, biochemistry, and localized biosensor development, and therefore continues to reveal unexpected findings.[42,43]

## RESOURCE AVAILABILITY

### Lead contact

Further information and requests for resources and reagents should be directed to and will be fulfilled by the lead contact, Corey Allard (corey_allard@hms.harvard.edu).

### Materials availability

Plasmids generated in this study are available upon request. No other unique reagents were generated in this study.

### Data and code availability

Sequencing data generated from this study are available at the NCBI Sequence Read Archive under BioProject: PRJNA1187635, accession numbers SRA: SAMN44801002, SAMN44801003, SAMN44801004, SAMN44801005, SAMN44801006, SAMN44801007, SAMN44801008, SAMN44801009, SAMN44801010, SAMN44801011, SAMN44801012, SAMN44801013, SAMN44801014, SAMN44801015, SAMN44801016, SAMN44801017, SAMN44801018, SAMN44801019, SAMN44801020, SAMN44801021, SAMN44801022, SAMN44801023, SAMN44801024, SAMN44801025, SAMN44801026, SAMN44801027, SAMN44801028, SAMN44801029, SAMN44801030, SAMN44801031. Any additional information required to reanalyze the data reported in this paper is available from the lead contact upon request.

## ACKNOWLEDGMENTS

We thank A. Grearson for photography; C. Heacock for experimental support; L. Soucy for scientific illustration; Dr. J. Widhalm for slugs, algae, and aquaculture advice; the Taplin mass spectrometry Core at Harvard Medical School; the Harvard Medical School Electron Microscopy Core Facility; and the Harvard Center for Biological Imaging (HCBI). This research was supported by the following funding sources: New York Stem Cell Foundation (N.W.B.), National Institutes of Health grant R35GM142697 (N.W.B.), Harvard Brain Initiative Postdoc Pioneer Award (C.A.H.A.), the Charles A. King Trust Postdoctoral Fellowship (C.A.H.A.), National Science Foundation grant PRFB2010728 (C.A.H.A.), The Mathers Foundation (A.S.Y.L.), National Institutes of Health R35GM142527 (A.S.Y.L.), National Science Foundation Graduate Research Fellowship NSF-GRFP 2019271478 (A.B.T.), Achievement Rewards for College Scientists Fellowship (A.B.T.), Company of Biologists grant JEBTF181124 (E.M.J.L.), Dutch Research Council project VI.Veni.202.218 (E.M.J.L.), and National Science Foundation grant PRFB2010971 (P.M.V.).

## AUTHOR CONTRIBUTIONS

Conceptualization, C.A.H.A., M.T., N.W.B., and A.S.Y.L.; methodology, C.A.H.A., A.B.T., P.M.V., M.T., and A.S.Y.L.; investigation, C.A.H.A., A.B.T., R.M., P.M.V., O.D.L., B.L.W., E.M.J.L., A.S.Y.L., and N.W.B.; visualization, C.A.H.A.; funding acquisition, N.W.B.; project administration, N.W.B.; supervision, C.A.H.A., M.T., and N.W.B.; writing – original draft, C.A.H.A. and N.W.B.; writing – review and editing, all authors.

## DECLARATION OF INTERESTS

The authors declare no competing interests.

## DECLARATION OF GENERATIVE AI AND AI-ASSISTED TECHNOLOGIES IN THE WRITING PROCESS

Generative AI and AI-assisted technologies were not used in the preparation or production of this manuscript.

Please cite this article in press as: Allard et al., A host organelle integrates stolen chloroplasts for animal photosynthesis, Cell (2025), https://doi.org/10.1016/j.cell.2025.06.003





## STAR★METHODS

Detailed methods are provided in the online version of this paper and include the following:

- KEY RESOURCES TABLE
- EXPERIMENTAL MODEL AND STUDY PARTICIPANT DETAILS
  - Animals
  - Cell Culture
- METHOD DETAILS
  - Starvation experiments
  - Transcriptomics
  - Cell transfection
  - Plastid Cell Dissociation
  - Chloroplast enrichment
  - Histology
  - Protein mass spectrometry
  - Electron microscopy
  - *In vivo* photosynthesis
  - Respirometry
  - Patch-clamp electrophysiology
  - Imaging Plastid Autofluorescence
- QUANTIFICATION AND STATISTICAL ANALYSIS

## SUPPLEMENTAL INFORMATION

Supplemental information can be found online at https://doi.org/10.1016/j.cell.2025.06.003.

Received: November 20, 2024
Revised: April 7, 2025
Accepted: June 3, 2025

## REFERENCES

1. Jensen, K.R. (1981). Observations on feeding methods in some florida ascoglossans. J. Molluscan Stud. *47*, 190–199. https://doi.org/10.1093/oxfordjournals.mollus.a065567.
2. Gallop, A., Bartrop, J., and Smith, D.C. (1980). The Biology of Chloroplast Acquisition by Elysia viridis. Proc. R. Soc. Lond. B *207*, 335–349.
3. Trench, R.K., Trench, M.E., and Muscatine, L. (1972). Symbiotic chloroplasts; their photosynthetic products and contribution to mucus synthesis in two marine slugs. Biol. Bull. *142*, 335–349. https://doi.org/10.2307/1540236.
4. Trench, R.K., Boyle, E.J., Smith, D.C., and Harley, J.L. (1973). The association between chloroplasts of Codium fragile and the mollusc Elysia viridis II. Chloroplast ultrastructure and photosynthetic carbon fixation in E. viridis. Proc. R. Soc. Lond. B. *184*, 63–81. https://doi.org/10.1098/rspb.1973.0031.
5. Kawaguti, S. (1965). Electron microscopy on the symbiosis between an elysioid gastropod and chloroplasts of a green alga. Biol. J. Okuyama Univ. *11*, 57–65.
6. Hinde, R., and Smith, D.C. (1972). Persistence of Functional Chloroplasts in Elysia viridis (Opisthobranchia, Sacoglossa). Nat. New Biol. *239*, 30–31. https://doi.org/10.1038/newbio239030a0.
7. Rumpho, M.E., Dastoor, F.P., Manhart, J.R., and Lee, J. (2007). The Kleptoplast. In The Structure and Function of Plastids, R.R. Wise and J.K. Hoober, eds. (Springer), pp. 451–473. https://doi.org/10.1007/978-1-4020-4061-0_23.
8. Green, B.J., Li, W.Y., Manhart, J.R., Fox, T.C., Summer, E.J., Kennedy, R.A., Pierce, S.K., and Rumpho, M.E. (2000). Mollusc-Algal Chloroplast Endosymbiosis. Photosynthesis, Thylakoid Protein Maintenance, and Chloroplast Gene Expression Continue for Many Months in the Absence of the Algal Nucleus1. Plant Physiol. *124*, 331–342. https://doi.org/10.1104/pp.124.1.331.
9. Mujer, C.V., Andrews, D.L., Manhart, J.R., Pierce, S.K., and Rumpho, M.E. (1996). Chloroplast genes are expressed during intracellular symbiotic association of Vaucheria litorea plastids with the sea slug Elysia chlorotica. Proc. Natl. Acad. Sci. USA *93*, 12333–12338. https://doi.org/10.1073/pnas.93.22.12333.
10. Christa, G., Zimorski, V., Woehle, C., Tielens, A.G.M., Wägele, H., Martin, W.F., and Gould, S.B. (2014). Plastid-bearing sea slugs fix CO2 in the light but do not require photosynthesis to survive. Proc. Biol. Sci. *281*, 20132493. https://doi.org/10.1098/rspb.2013.2493.
11. Cartaxana, P., Trampe, E., Kühl, M., and Cruz, S. (2017). Kleptoplast photosynthesis is nutritionally relevant in the sea slug Elysia viridis. Sci. Rep. *7*, 7714. https://doi.org/10.1038/s41598-017-08002-0.
12. Cartaxana, P., Rey, F., LeKieffre, C., Lopes, D., Hubas, C., Spangenberg, J.E., Escrig, S., Jesus, B., Calado, G., Domingues, R., et al. (2021). Photosynthesis from stolen chloroplasts can support sea slug reproductive fitness. Proc. Biol. Sci. *288*, 20211779. https://doi.org/10.1098/rspb.2021.1779.
13. Havurinne, V., and Tyystjärvi, E. (2020). Photosynthetic sea slugs induce protective changes to the light reactions of the chloroplasts they steal from algae. eLife *9*, e57389. https://doi.org/10.7554/eLife.57389.
14. Frankenbach, S., Melo Clavijo, J., Brück, M., Bleidißel, S., Simon, M., Gasparoni, G., Lo Porto, C., Laetz, E.M.J., Greve, C., Donath, A., et al. (2023). Shedding light on starvation in darkness in the plastid-bearing sea slug Elysia viridis (Montagu, 1804). Mar. Biol. *170*, 89. https://doi.org/10.1007/s00227-023-04225-0.
15. Cruz, S., LeKieffre, C., Cartaxana, P., Hubas, C., Thiney, N., Jakobsen, S., Escrig, S., Jesus, B., Kühl, M., Calado, R., et al. (2020). Functional kleptoplasts intermediate incorporation of carbon and nitrogen in cells of the Sacoglossa sea slug Elysia viridis. Sci. Rep. *10*, 10548. https://doi.org/10.1038/s41598-020-66909-7.
16. Laetz, E.M.J., Moris, V.C., Moritz, L., Haubrich, A.N., and Wägele, H. (2017). Photosynthate accumulation in solar-powered sea slugs - starving slugs survive due to accumulated starch reserves. Front. Zool. *14*, 4. https://doi.org/10.1186/s12983-016-0186-5.
17. Burgués Palau, L., Senna, G., and Laetz, E.M.J. (2024). Crawl away from the light! Assessing behavioral and physiological photoprotective mechanisms in tropical solar-powered sea slugs exposed to natural light intensities. Mar. Biol. *171*, 50. https://doi.org/10.1007/s00227-023-04350-w.
18. Evertsen, J., Burghardt, I., Johnsen, G., and Wägele, H. (2007). Retention of functional chloroplasts in some sacoglossans from the Indo-Pacific and Mediterranean. Mar. Biol. *151*, 2159–2166. https://doi.org/10.1007/s00227-007-0648-6.
19. Händeler, K., Grzymbowski, Y.P., Krug, P.J., and Wägele, H. (2009). Functional chloroplasts in metazoan cells - a unique evolutionary strategy in animal life. Front. Zool. *6*, 28. https://doi.org/10.1186/1742-9994-6-28.
20. Maeda, T., Takahashi, S., Yoshida, T., Shimamura, S., Takaki, Y., Nagai, Y., Toyoda, A., Suzuki, Y., Arimoto, A., Ishii, H., et al. (2021). Chloroplast acquisition without the gene transfer in kleptoplastic sea slugs, Plakobranchus ocellatus. eLife *10*, e60176. https://doi.org/10.7554/eLife.60176.
21. Ropolo, A., Grasso, D., Pardo, R., Sacchetti, M.L., Archange, C., Lo Re, A.L., Seux, M., Nowak, J., Gonzalez, C.D., Iovanna, J.L., et al. (2007). The Pancreatitis-induced Vacuole Membrane Protein 1 Triggers Autophagy in Mammalian Cells. J. Biol. Chem. *282*, 37124–37133. https://doi.org/10.1074/jbc.M706956200.
22. Dusetti, N.J., Jiang, Y., Vaccaro, M.I., Tomasini, R., Azizi Samir, A., Calvo, E.L., Ropolo, A., Fiedler, F., Mallo, G.V., Dagorn, J.-C., et al. (2002). Cloning and Expression of the Rat Vacuole Membrane Protein 1 (VMP1), a New Gene Activated in Pancreas with Acute Pancreatitis, Which Promotes Vacuole Formation. Biochem. Biophys. Res. Commun. *290*, 641–649. https://doi.org/10.1006/bbrc.2001.6244.
23. Li, J., and Lee, A.S. (2006). Stress Induction of GRP78/BiP and Its Role in Cancer. Curr. Mol. Med. *6*, 45–54. https://doi.org/10.2174/156652406775574523.

Please cite this article in press as: Allard et al., A host organelle integrates stolen chloroplasts for animal photosynthesis, Cell (2025), https://doi.org/10.1016/j.cell.2025.06.003



24. Martin, R., Walther, P., and Tomaschko, K.-H. (2013). Phagocytosis of algal chloroplasts by digestive gland cells in the photosynthesis-capable slug Elysia timida (Mollusca, Opisthobranchia, Sacoglossa). Zoomorphology *132*, 253–259. https://doi.org/10.1007/s00435-012-0184-x.

25. Curtis, N.E., Schwartz, J.A., and Pierce, S.K. (2010). Ultrastructure of sequestered chloroplasts in sacoglossan gastropods with differing abilities for plastid uptake and maintenance. Invertebr. Biol. *129*, 297–308. https://doi.org/10.1111/j.1744-7410.2010.00206.x.

26. Marin, A., and Ros, J. (1989). The chloroplast-animal association in four Iberian sacoglossan opisthobranchs: Elysia timida, Elysia translucens, Thuridilla hopei and Bosellia mimetica. Scientia mar *53*, 429–440.

27. Brandley, B.K. (1981). Ultrastructure of the Envelope of Codium a Ustralicum (silva) Chloroplasts in the Alga and After Acquisition by Elysia Maoria (powell). New Phytol. *89*, 679–686. https://doi.org/10.1111/j.1469-8137.1981.tb02346.x.

28. Marín, A., and Ros, J. (1993). ULTRASTRUCTURAL AND ECOLOGICAL ASPECTS OF THE DEVELOPMENT OF CHLOROPLAST RETENTION IN THE SACOGLOSSAN GASTROPOD ELYSIA TIMIDA. J. Molluscan Stud. *59*, 95–104. https://doi.org/10.1093/mollus/59.1.95.

29. Curtis, N.E., Massey, S.E., and Pierce, S.K. (2006). The symbiotic chloroplasts in the sacoglossan Elysia clarki are from several algal species. Invertebr. Biol. *125*, 336–345. https://doi.org/10.1111/j.1744-7410.2006.00065.x.

30. Laetz, E.M.J., Rühr, P.T., Bartolomaeus, T., Preisfeld, A., and Wägele, H. (2017). Examining the retention of functional kleptoplasts and digestive activity in sacoglossan sea slugs. Org. Divers. Evol. *17*, 87–99. https://doi.org/10.1007/s13127-016-0308-0.

31. Barott, K.L., Venn, A.A., Perez, S.O., Tambutté, S., and Tresguerres, M. (2015). Coral host cells acidify symbiotic algal microenvironment to promote photosynthesis. Proc. Natl. Acad. Sci. USA *112*, 607–612. https://doi.org/10.1073/pnas.1413483112.

32. Thies, A.B., Quijada-Rodriguez, A.R., Zhouyao, H., Weihrauch, D., and Tresguerres, M. (2022). A Rhesus channel in the coral symbiosome membrane suggests a novel mechanism to regulate NH3 and CO2 delivery to algal symbionts. Sci. Adv. *8*, eabm0303. https://doi.org/10.1126/sciadv.abm0303.

33. Yonge, C.M. (1931). The Significance of the Relationship between Corals and Zooxanthellæ. Nature *128*, 309–311. https://doi.org/10.1038/128309a0.

34. Wooldridge, S.A. (2010). Is the coral-algae symbiosis really "mutually beneficial" for the partners? BioEssays *32*, 615–625. https://doi.org/10.1002/bies.200900182.

35. Muscatine, L., Pool, R.R., and Trench, R.K. (1975). Symbiosis of Algae and Invertebrates: Aspects of the Symbiont Surface and the Host-Symbiont Interface. Trans. Am. Microsc. Soc. *94*, 450–469. https://doi.org/10.2307/3225518.

36. Wiedenmann, J., D'Angelo, C., Mardones, M.L., Moore, S., Benkwitt, C.E., Graham, N.A.J., Hambach, B., Wilson, P.A., Vanstone, J., Eyal, G., et al. (2023). Reef-building corals farm and feed on their photosynthetic symbionts. Nature *620*, 1018–1024. https://doi.org/10.1038/s41586-023-06442-5.

37. Colley, N.J., and Trench, R.K. (1985). Cellular events in the reestablishment of a symbiosis between a marine dinoflagellate and a coelenterate. Cell Tissue Res. *239*, 93–103. https://doi.org/10.1007/BF00214908.

38. Fitt, W.K., and Trench, R.K. (1983). Endocytosis of the symbiotic dinoflagellate Symbiodinium microadriaticum Freudenthal by endodermal cells of the scyphistomae of Cassiopeia xamachana and resistance of the algae to host digestion. J. Cell Sci. *64*, 195–212. https://doi.org/10.1242/jcs.64.1.195.

39. Chen, M.-C., Cheng, Y.-M., Sung, P.-J., Kuo, C.-E., and Fang, L.-S. (2003). Molecular identification of Rab7 (ApRab7) in Aiptasia pulchella and its exclusion from phagosomes harboring zooxanthellae. Biochem. Biophys. Res. Commun. *308*, 586–595. https://doi.org/10.1016/s0006-291x(03)01428-1.

40. Baird, A.H., Bhagooli, R., Ralph, P.J., and Takahashi, S. (2009). Coral bleaching: the role of the host. Trends Ecol. Evol. *24*, 16–20. https://doi.org/10.1016/j.tree.2008.09.005.

41. de Vries, J., Habicht, J., Woehle, C., Huang, C., Christa, G., Wägele, H., Nickelsen, J., Martin, W.F., and Gould, S.B. (2013). Is ftsH the Key to Plastid Longevity in Sacoglossan Slugs? Genome Biol. Evol. *5*, 2540–2548. https://doi.org/10.1093/gbe/evt205.

42. Mindell, J.A. (2012). Lysosomal Acidification Mechanisms. Annu. Rev. Physiol. *74*, 69–86. https://doi.org/10.1146/annurev-physiol-012110-142317.

43. Accardi, A. (2021). Not so transport incompetent after all: Revisiting a CLC-7 mutant sheds new mechanistic light on lysosomal physiology. J. Gen. Physiol. *153*, e202012805. https://doi.org/10.1085/jgp.202012805.

44. Buchfink, B., Reuter, K., and Drost, H.-G. (2021). Sensitive protein alignments at tree-of-life scale using DIAMOND. Nat. Methods *18*, 366–368. https://doi.org/10.1038/s41592-021-01101-x.

45. Grabherr, M.G., Haas, B.J., Yassour, M., Levin, J.Z., Thompson, D.A., Amit, I., Adiconis, X., Fan, L., Raychowdhury, R., Zeng, Q., et al. (2011). Trinity: reconstructing a full-length transcriptome without a genome from RNA-Seq data. Nat. Biotechnol. *29*, 644–652. https://doi.org/10.1038/nbt.1883.

46. Bray, N.L., Pimentel, H., Melsted, P., and Pachter, L. (2016). Near-optimal probabilistic RNA-seq quantification. Nat. Biotechnol. *34*, 525–527. https://doi.org/10.1038/nbt.3519.

47. Krueger, F., James, F., Ewels, P., Afyounian, E., Weinstein, M., Schuster-Boeckler, B., Hulselmans, G., and sclamons. (2023). FelixKrueger/TrimGalore: v0.6.10 - add default decompression path. Zenodo. https://doi.org/10.5281/zenodo.7598955.

48. The UniProt Consortium (2015). UniProt: a hub for protein information. Nucleic Acids Res. *43*, D204–D212. https://doi.org/10.1093/nar/gku989.

49. Soneson, C., Love, M.I., and Robinson, M.D. (2015). Differential analyses for RNA-seq: transcript-level estimates improve gene-level inferences. F1000Res *4*, 1521. https://doi.org/10.12688/f1000research.7563.2.

50. Ma, Y., McClatchy, D.B., Barkallah, S., Wood, W.W., and Yates, J.R. (2018). Quantitative analysis of newly synthesized proteins. Nat. Protoc. *13*, 1744–1762. https://doi.org/10.1038/s41596-018-0012-y.

51. Rappsilber, J., Ishihama, Y., and Mann, M. (2003). Stop and Go Extraction Tips for Matrix-Assisted Laser Desorption/Ionization, Nanoelectrospray, and LC/MS Sample Pretreatment in Proteomics. Anal. Chem. *75*, 663–670. https://doi.org/10.1021/ac026117i.

52. Peng, J., and Gygi, S.P. (2001). Proteomics: the move to mixtures. J. Mass Spectrom. *36*, 1083–1091. https://doi.org/10.1002/jms.229.

53. Eng, J.K., McCormack, A.L., and Yates, J.R. (1994). An approach to correlate tandem mass spectral data of peptides with amino acid sequences in a protein database. J. Am. Soc. Mass Spectrom. *5*, 976–989. https://doi.org/10.1016/1044-0305(94)80016-2.

Please cite this article in press as: Allard et al., A host organelle integrates stolen chloroplasts for animal photosynthesis, Cell (2025), https://doi.org/10.1016/j.cell.2025.06.003



CellPress

## STAR★METHODS

### KEY RESOURCES TABLE

| REAGENT or RESOURCE | SOURCE | IDENTIFIER |
|---|---|---|
| **Antibodies** | | |
| rabbit anti-Phospho-4E-BP1 (Thr37/46) | Cell Signaling Technology | Cat#2855 |
| mouse anti-Tubulin | Developmental Studies Hybridoma Bank | Cat#E7 |
| goat anti-P2X4 | Novus | Cat#NBP2-27567 |
| rabbit anti-Rab7a | Novus | Cat#NBP2-24591 |
| Rabbit anti-VHA | Barrot et al.[31] | N/A |
| NPC2 | Novus | Cat#NBP1-52028 |
| goat anti-rabbit IgG H&L (Alexa Fluor® 488) | AbCam | Cat#ab6702 |
| goat anti-mouse IgG H&L (Cy3 ®) | AbCam | Cat#ab97035 |
| IRDye® 800CW goat anti-rabbit IgG | Licor Biosciences | Cat#926-32211 |
| IRDye® 680RD goat anti-mouse IgG | Licor Biosciences | Cat#926-68070 |
| donkey anti-goat IgG H&L Alexa Fluor® 555 | AbCam | Cat#A-21432 |
| anti-FLAG®M2 monoclonal antibody | Sigma | Cat#F1804 |
| **Chemicals, peptides, and recombinant proteins** | | |
| FM1-84 | Invitrogen | Cat#T3163 |
| Ivermectin | MedChemExpress | Cat#HY-15310 |
| 5-BDBD | Tocris | Cat#3579 |
| DCMU | Sigma | Cat#D2425 |
| BODIPY™ 505/515 | Invitrogen | Cat#D3921 |
| Torin-1 | Selleck Chemicals | Cat#S2827 |
| Suramin hexasodium salt | Tocris | Cat#1472 |
| PPADS tetrasodium salt | Tocris | Cat#0625 |
| LysoTracker™ Red DND-99 | Invitrogen | Cat#L7528 |
| Click-IT™ AHA | Invitrogen | Cat#C10102 |
| protease type XIV | Sigma | Cat#9036-06-0 |
| lysozyme | Sigma | Cat#12650-88-3 |
| **Deposited data** | | |
| RNA-seq reads | This study | BioProject: PRJNA1187635, accession numbers: SAMN44801002, SAMN44801003, SAMN44801004, SAMN44801005, SAMN44801006, SAMN44801007, SAMN44801008, SAMN44801009, SAMN44801010, SAMN44801011, SAMN44801012, SAMN44801013, SAMN44801014, SAMN44801015, SAMN44801016, SAMN44801017, SAMN44801018, SAMN44801019, SAMN44801020, SAMN44801021, SAMN44801022, SAMN44801023, SAMN44801024, SAMN44801025, SAMN44801026, SAMN44801027, SAMN44801028, SAMN44801029, SAMN44801030, SAMN44801031 |

(*Continued on next page*)

Please cite this article in press as: Allard et al., A host organelle integrates stolen chloroplasts for animal photosynthesis, Cell (2025), https://doi.org/10.1016/j.cell.2025.06.003



*Continued*

| REAGENT or RESOURCE | SOURCE | IDENTIFIER |
|---|---|---|
| Experimental Models: Cell lines | | |
| HEK293T cellls | ATCC | Cat#CRL-1573 |
| Experimental models: Organisms/strains | | |
| *Elysia clarkiii* | LiveAquaria/Carolina Biological Supply | N/A |
| *Aplysia californica* | National Resource for Aplysia, University of Miami | N/A |
| Exaiptasia diaphana | Carolina Biological Supply | N/A |
| Lobophytum sp. | LiveAquaria | N/A |
| Recombinant DNA | | |
| Plasmid: pUNIV-P2X4-GFP (*Elysia clarkii*) | Genscript | N/A |
| Plasmid: pUNIV-P2X4-GFP (H | Genscript | N/A |
| Plasmid: pUNIV-Rab7-FLAG (*Human*) | Genscript | N/A |
| Plasmid: pUNIV-Rab7-FLAG (*Aplysia californica*) | Genscript | N/A |
| Plasmid: pUNIV-Rab5-FLAG (*Elysia clarkii*) | Genscript | N/A |
| Plasmid: pUNIV-Rab7-FLAG (*Elysia clarkii*) | Genscript | N/A |
| Plasmid: pUNIV-Rab9-FLAG (*Elysia clarkii*) | Genscript | N/A |
| Plasmid: LAMP1-GFP | Addgene | Cat#16290 |
| Software and algorithms | | |
| Diamond v.2.0.9 | Buchfink et al.[44] | https://github.com/bbuchfink/diamond |
| Trinity v.2.4.0 | Grabherr et al.[45] | https://github.com/trinityrnaseq/trinityrnaseq |
| Kallisto | Bray et al.[46] | https://github.com/pachterlab/kallisto |
| ImageJ2/FIJI | NIH | https://imagej.net/software/fiji/downloads |
| pClamp v.11.3 | Axon Instruments | N/A |
| ClampFit v.11.3 | Axon Instruments | N/A |
| Prism v.10 | GraphPad | https://www.graphpad.com/features |
| SensorTrace v.3.4.3 | Unisense | https://unisense.com/software-download/ |

## EXPERIMENTAL MODEL AND STUDY PARTICIPANT DETAILS

### Animals

Photosynthetic sea slugs (*Elysia crispata*, *clarki* subtype) were supplied from LiveAquaria or Carolina Biological Supply and housed in 40 L glass aquaria containing aerated natural sea water kept at 26 °C and provided with *Bryopsis*, *Penicillus* and *Halimeda* algae as food source.[29] Sea hares (*Aplysia californica*), *which can grow larger than Elysia slugs*, were sourced from the National Resource for Aplysia at the University of Miami and housed in 40 L glass aquaria containing aerated natural sea water kept at room temperature and fed *Agardhiella subulate*. *Exaiptasia diaphana* were sourced from Carolina Biological Supply and housed in 40 L glass aquaria containing aerated natural sea water kept at 26 °C and fed brine shrimp 3X weekly. Corals were purchased from LiveAquaria and used immediately for experiments. Animals were under a Satellite Pro Plus LED lamp with PAR range of 150-400 from the bottom to the top of the tank, respectively. Lights were kept on a 14:10 light-dark cycle. Sacoglossan sea slugs are simultaneous hermaphrodites, and the age of the organisms is unknown.

### Cell Culture

HEK293 cells (ATCC, authenticated and validated as negative for mycoplasma by vendor) were cultured in Dulbecco's Modified Eagle Medium (DMEM) (Gibco) supplemented with 10% fetal calf serum (FBS) (Gibco) and 50 I.U./mL penicillin and 50 μg/mL streptomycin (Gibco) at 37 °C, 5% $CO_2$ using standard techniques.

Please cite this article in press as: Allard et al., A host organelle integrates stolen chloroplasts for animal photosynthesis, Cell (2025), https://doi.org/10.1016/j.cell.2025.06.003





## METHOD DETAILS

### Starvation experiments

Animals were housed as above but without food. Mortality was checked daily by gently prodding any animal that appeared dead to check for response. In a separate experiment, 3 animals were collected at each week of starvation and frozen in RNAlater at -80 °C for subsequent RNA sequencing experiments.

### Transcriptomics

We generated *de novo* transcriptomes for *Elysia crispata* and *Aplysia californica*. Using samples from starvation experiments frozen in RNAlater: RNA extraction, library preparation, and RNA sequencing were performed by Genewiz (Azenta) using a HiSeq (2 x 150 bp) platform. Adaptor trimming was performed using trimgalore,[47] and reference transcriptomes were assembled de novo using Trinity.[45] Open reading frames were identified using transdecoder.[45] Reads were pseudo-aligned and transcript abundance was estimated using Kallisto[46] and our novel transcriptome assemblies as a reference. Annotation was performed using Diamond.[44]

To quantify animal and plant-specific transcripts separately, different reference databases (Metazoa- Taxon ID:22308 and plant-Taxon ID:33090) were assembled from Universal Protein Resource (UniProt)[48] using the Diamond[44] makedb command. Transcript level information from Kallisto was collapsed across isoforms using tximport[49]) for gene level analysis. Genes of interest were batch mapped to their respective Gene Ontology (GO) categories in Uniprot and subsequently analysed with a custom Python script. Sequencing data generated from this study are available at the NCBI Sequence Read Archive under BioProject: PRJNA1187635, accession numbers SRA: SAMN44801002-SAMN44801031.

### Cell transfection

HEK293T or AD293 cells were washed with Opti-MEM Reduced Serum Media (Gibco) and incubated with transfection mix containing 1 μg total of the indicated plasmid DNA and 3 μL Lipofectamine 3000 Transfection Reagent (Invitrogen) in Opti-MEM for 4-8 hours at 37 °C. Cells were then replated onto glass coverslips in supplemented DMEM, incubated for 2 hr at 37 °C, and then moved to 30 °C incubation overnight.

### Plastid Cell Dissociation

Individual slugs were sacrificed by rapid decapitation and cut into small pieces, which were incubated in artificial seawater (ASW) (430 mM NaCl, 10 mM KCl, 10 mM HEPES, 10 mM $CaCl_2$, 50 mM $MgCl_2$, pH 7.6) containing 10 mM D-glucose, 10mg/mL protease type XIV (Sigma #9036-06-0) and 10 mg/mL lysozyme (Sigma #12650-88-3). Tissue was incubated at 30 °C for 15 minutes, enzyme solution was removed, and replaced with fresh artificial seawater with glucose containing 0.05% bovine serum albumin (BSA). Tissue was triturated with a micropipette and periodically checked under a microscope until tissue was broken up into a single cell suspension.

### Chloroplast enrichment

Individual slugs were sacrificed by rapid decapitation and cut into small pieces several millimeters long. Slug tissue pieces were submerged in 30% (v/v) ethanol for 1 min, then moved to ice cold chloroplast buffer (in mM, 500 Sucrose, 50 HEPES, 15 $MgCl_2$, pH 7.8) containing 2 mg/mL BSA and 10 mg/mL lysozyme. Tissue pieces were lysed in 1 mL of chloroplast buffer in a dounce homogenizer, keeping the buffer to tissue ratio 10:1. Slug homogenates were incubated at room temp with occasional vortexing for 10 mins to allow lysozyme to digest the slug mucous. Samples were then combined, filtered through a 100 μm cell strainer, and centrifuged at 100 x g. The supernatant containing chloroplasts was transferred to a new tube and centrifuged at 1,500 x g at 4 °C for 5 mins to pellet chloroplasts. The supernatant was then removed and replaced with 1-2 mL chloroplast buffer. Intact chloroplasts were isolated on discontinuous Percoll density gradients (50% to 10% in 10% steps). A 100% Percoll solution was first made by combining 10 mL Percoll, 0.1 g Ficoll 400, 0.5 g PEG 6000, 3.42 g Sucrose, and 40 mg BSA. This 100% solution was diluted to 50% using dilution buffer (in mM, 30 $MgCl_2$, 100 HEPES), and 50% solution was further diluted in chloroplast buffer to make each gradient. After gradients were prepared, 1-2 mL of intact chloroplast suspension was layered on each gradient and centrifuged at 3,500 x g for 30 mins at 4 °C with the brake off. Following centrifugation, the band present at the 40-50% interface contained intact chloroplasts. The upper layers were aspirated away to recover the chloroplast layer, which was distributed in 0.1 mL aliquots and diluted in 1 mL of chloroplast buffer. Each aliquot was spun at 1,500 x g for 5 mins to pellet chloroplasts and remove residual Percoll solution. All pellets were combined into a single tube, washed twice with chloroplast buffer without BSA or lysozyme, flash frozen in liquid nitrogen, and stored at -80 °C.

### Histology

#### *Thin Section*

Tissues from the indicated species were fixed in 4% paraformaldehyde (PFA) in ASW for approximately 12 hr at 4 °C, dissected into small sections, washed with phosphate-buffered saline (PBS), and embedded in OCT (optimal cutting temperature compound). After embedding, samples were frozen and sectioned using a cryostat (Leica CM3050S) at 18-20 μm sections and mounted on Superfrost slides (Fischer Scientific). After two washes in PBS, samples were blocked for 20 minutes in 5% normal goat serum (NGS) and 0.1% Triton X-100 in PBS, or 5% normal donkey serum (NDS) and 0.1% Triton X-100 in PBS. After washing twice with PBS, the primary

Please cite this article in press as: Allard et al., A host organelle integrates stolen chloroplasts for animal photosynthesis, Cell (2025), https://doi.org/10.1016/j.cell.2025.06.003



antibody solutions, composed of either 1% rabbit anti-Rab7 (Novus #NBP2-24591), goat anti-P2x4 (Novus #NBP2-27567), rabbit anti-VHA,[31] or goat anti-NPC2 (Novus #NBP1-52028) and 0.1% Triton X-100 in PBS were applied to the samples and left for 12 hr at 4°C. Samples were then washed with PBS 3 times and secondary antibody mix containing goat anti-rabbit IgG H&L (Alexa Fluor® 488) (Abcam ab6702) or donkey Anti-goat IgG H&L (Alexa Fluor® 488) (Abcam ab150129) was added to the respective samples (1:500) in PBS with 0.1% Triton X-100. Finally, the samples were washed 3 times in PBS, mounted in Vectashield with DAPI (Vector Laboratories), and imaged with a LSM 900 Confocal Microscope (Zeiss). Images were processed using FIJI.

### Immunofluorescence staining of HEK Cells

HEK293T cells were transfected as described above. Cells were washed 3 times in PBS and fixed in 4% paraformaldehyde (PFA) in PBS for 10 min at room temperature. Coverslips were then incubated in blocking mixture containing 1% bovine serum albumin (BSA) and 10 mM glycine in PBS. Samples were then incubated in antibody solution containing goat anti-P2x4 (Novus #NBP2-27567) for 24 hr at 4 °C in PBS containing 1% BSA. Samples were then washed with PBS 3 times, and secondary antibody mix containing donkey anti-goat IgG H&L Alexa Fluor® 555 (Abcam #A-21432) (1:500) was added. Finally, the samples were washed 3 times in PBS, mounted in Vectashield with DAPI (Vector Laboratories), and imaged with a LSM 980 Confocal Microscope with Airyscan2 (Zeiss). Images were processed using FIJI.

### Dissociated kleptosomes

Kleptosomes were dissociated as for plastid cells, but isolated plastid cells were then disrupted by repeated passage through a 20-gauge syringe. Dissociated kleptoplasts were plated on poly-lysine coated dishes, and antibody staining was performed as described for thin section histology. Kleptosomes were imaged in PBS with an LSM 980 Confocal Microscope with Airyscan2 (Zeiss). Images were processed using FIJI.

### Nucleoids

Dissociated plastid cells were stained with Hoechst 33342 solution (Abcam # ab228551) diluted to 5μM in artificial sea water, mounted on poly-lysine coated glass-bottom dishes, and imaged with a LSM 900 Confocal Microscope (Zeiss).

### BODIPY and Lysotracker stain

Individual slugs were sacrificed by rapid decapitation and cut into small pieces several millimeters long and embedded in OCT, frozen, and sectioned using a cryostat (Leica CM3050S) at 18-20 μm sections and mounted on Superfrost slides (Fischer Scientific). Tissue sections were washed twice in ASW, and then stained using 5 μM BODIPY™ 505/515 (4,4-Difluoro-1,3,5,7-Tetramethyl-4-Bora-3a,4a-Diaza-s-Indacene) (Invitrogen #D3921) or 1 μM Lysotracker™ Red DND-99 (Invitrogen #L7528) in ASW for ten minutes, washed twice in ASW, mounted in ASW, and imaged with a LSM 980 Confocal Microscope with Airyscan2 (Zeiss). For dissociated cells and kleptoplasts, tissues were dissociated as above except the 1μM Lysotracker Green DND-26 (Invitrogen #L7526) was added to the enzyme solution.

### FM1-43 staining

Tissue sections, dissociated cells, and organelles were stained using 5 μg/mL FM1-43 (Invitrogen #T3163) in ASW for five minutes, rinsed twice in ASW, and used for down-stream experiments including patch-clamp and imaging.

### Nascent protein labeling and click chemistry

To measure nascent protein synthesis in slugs and sequestered chloroplasts, we employed biorthogonal non-canonical amino acid tagging (BONCAT) and the click reaction to label new proteins.[50] Slugs were incubated in 60 mL of 5 mM L-azidohomoalanine (AHA) (Invitrogen # C10102) in seawater for 6 hours under bright light (PAR ~400) in a 26°C incubator. Following incubation, intact chloroplasts were purified from slug tissue as described above and proteins were then extracted using radioimmunoprecipitation assay buffer (150 mM NaCl, 50 mM Tris pH 8.0, 1% Triton X-100, 0.5% sodium deoxycholate, 0.1% sodium dodecyl sulfate, 1 mM phenylmethylsulfonyl fluoride, and one cOmplete EDTA-free protease inhibitor cocktail tablet (Roche #11697498001) per 25 mL buffer) and quantified using a Pierce BCA protein assay kit (ThermoScientific #23225). To perform the click reaction, 100 μg of protein were resuspended in PBS, and the following components were added to a final concentration in order: 100 μM TBTA, 1 mM CuSO4, 100 μM biotin-alkyne, and 1 mM TCEP. Final reaction volume was 100 μL, and samples were incubated end-over-end for 1 hour at room temp. Following the click reaction, proteins were recovered by methanol-chloroform precipitation and protein pellets were resuspended in PBS with 0.1% NP-40.

### SDS-PAGE and Western Blotting

*Click-chemistry:* Labeled and unlabeled proteins (~10 μg) were diluted in 2x Laemmli buffer, heated to 95 °C for 5 mins, loaded in equimolar quantities on precast Any kD Mini-PROTEAN gels (Bio-Rad #4569036), and subjected to gel electrophoresis in SDS-PAGE buffer (25 mM tris, 192 mM glycine, 0.1% SDS, pH 8.3) at 150 V for 1 hour. Total protein was visualized by Coomassie stain (Bio-Rad #1610435) and imaged using an Azure Biosystems c200 gel imaging system. For AHA-directed Western blots, gels were transferred to 0.2 μm nitrocellulose membrane using the Trans-Blot Turbo transfer system (Bio-Rad #1704150). Membranes were incubated for 30 min in Intercept® (TBS) Blocking Buffer (LI-COR Biosciences #927-60003) and then incubated with conjugated streptavidin primary antibody (LI-COR Biosciences #926-32230) diluted to 1% in Intercept® T20 (TBS) Antibody Diluent (LI-COR Biosciences #927-65001) and incubated overnight at 4 °C. The following day, membranes were washed 3x with tris-buffered saline (TBS) and imaged on a LI-COR Odyssey DLx imaging system.

*mTOR activity immunoblotting:* Individual slugs were sacrificed by rapid decapitation and immediately dropped into liquid nitrogen, ground into powder using a chilled coffee-grinder. Powder was weighed and resuspended in an equivalent volume (w/v) of lysis buffer (20 mM Tris, 150 mM NaCl, 20 mM NaF, 50 mM sodium orthovanadate, 50 mM beta-glycerophosphate, 1 mM

Please cite this article in press as: Allard et al., A host organelle integrates stolen chloroplasts for animal photosynthesis, Cell (2025), https://doi.org/10.1016/j.cell.2025.06.003



phenylmethanesulfonyl fluoride, and 1X cOmplete™ Protease Inhibitor Cocktail (Roche), pH 7.4). Samples were homogenized by bead-beating at 4 °C for 2 min, and supernatants were mixed 1:1 (v/v) in 2X Laemmli buffer, boiled at 95 °C, centrifuged at 10,000 x g for 2 minutes, and supernatants were collected for western blotting.

Western blot samples were loaded onto 4-20% polyacrylamide gradient gels (Bio-Rad # 4561094) along with a pre-stained ladder (Chameleon Duo, LI-COR Biosciences # 928-60000) and electrophoresis was run at a constant 100 V. Detection of p4E-BP1 in samples from Elysia slugs was difficult and required the gel to be run carefully until the 15 kDa band was nearly run off the gel to remove as much of the green chlorophyll pigment from the gel as possible, which is extremely autofluorescent in the near-IR detection range of the imaging system and could easily mask the signal from the antibody. Proteins were then transferred to nitrocellulose for blotting using mixed-molecular weight settings on a Turbo Blot transfer system (Bio-Rad #1704150). Gels were blocked in Odyssey Blocking Solution (LI-COR Biosciences #927–60001) for 30 min, incubated in primary antibody mix containing rabbit anti-Phospho-4E-BP1 (Thr37/46) (236B4) monoclonal antibody (Cell Signaling Technology #2855) diluted 1:1000 and mouse anti-Tubulin monoclonal antibody (Sigma # T7451) I diluted 1:10,000 in Intercept T-20 Antibody Diluent (LI-COR Biosciences #927–65001) overnight at 4 °C, washed 3X in TBS, incubated for 1 hour at 25 °C in secondary antibody mix containing IRDye® 800CW Goat anti-Rabbit IgG secondary antibody (LICOR Biosciences #926-32211) and IRDye® 680RD Goat anti-Mouse IgG Secondary Antibody (LICOR Biosciences #926-68070) diluted 1:10,000 in Intercept T-20 Antibody Diluent, and finally washed 3 times in TBS before imaging. Use of the 800 channel for detecting phospho-4E-BP1 was critical given lower autofluorescence from chlorophyll in this channel. Western blots were imaged using an Odyssey CLx imaging system (LI-COR Biosciences) and processed using Image Studio (LI-COR Biosciences). Detection of p4E-BP1 in Aplysia was considerably easier likely because Elysia lysates produce copious amounts of mucus and autofluorescent pigments. We therefore limit our discussion to the kinetics of P-4EBP1 reduction in the context of what we can reliably measure, namely that P4EBP1 levels drop within a week of food deprivation in both species, suggesting they both enter some level of starvation within a similar time course.

For Torin-1 treatment controls, live animals were incubated in 500mL beakers containing sea water, food algae, and 0.1% DMSO or 2.5μM Torin-1 (Selleck Chemicals #S2827) in 0.1% DMSO for 24 hours before samples were collected for western blotting as above.

*Rab7 immunoblotting:* HEK293T cells transiently transfected with plasmids expressing the indicate Rab proteins (35 mm dish, 95% confluency) were resuspended and washed twice in TBS and lysed in 100 μL lysis buffer (20 mM Tris, 150 mM NaCl, 1 mM phenylmethanesulfonyl fluoride, and 1X cOmplete™ Protease Inhibitor Cocktail (Roche), pH 7.4, 1% Triton-X 100). Lysates were cleared by centrifugation at 10,000 x g for 2 minutes, and the supernatant was mixed 1:1 in 2X Laemmli buffer, boiled, and loaded onto 4-20% polyacrylamide gradient gels (Bio-Rad # 4561094) along with a pre-stained ladder (Chameleon Duo, LI-COR Biosciences # 928-60000) and electrophoresis was run at a constant 150 V until the dye front was run off the gel. Proteins were then transferred to nitrocellulose for blotting using mixed-molecular weight settings on a Turbo Blot transfer system (Bio-Rad #1704150). Gels were blocked in Odyssey Blocking Solution (LI-COR Biosciences #927–60001) for 30 min, incubated in primary antibody mix containing either (1) rabbit anti-Rab7 polyclonal antibody (Novus # NBP2-24591) diluted 1:1000 and mouse ANTI-FLAG® M2 monoclonal antibody (Sigma # F1804) diluted 1:3,000 in Intercept T-20 Antibody Diluent (LI-COR Biosciences #927–65001) overnight at 4 °C, washed 3X in TBS, incubated for 1 hour at 25 °C in secondary antibody mix containing IRDye® 800CW Goat anti-Rabbit IgG secondary antibody (LI-COR Biosciences #926-32211) and IRDye® 680RD Goat anti-Mouse IgG Secondary Antibody (LI-COR Biosciences #926-68070) diluted 1:10,000 in Intercept T-20 Antibody Diluent, and finally washed 3 times in TBS before imaging. Western blots were imaged using an Odyssey CLx imaging system (LI-COR Biosciences) and processed using Image Studio (LI-COR Biosciences).

## Protein mass spectrometry

Nascent protein identification was performed with the Taplin Mass Spectrometry Facility at Harvard Medical School. Briefly, AHA-labeled proteins were immunoprecipitated overnight using magnetic streptavidin beads in pulldown buffer (20 mM Tris-HCl, 100 mM NaCl, 10 mM $MgCl_2$, 0.1% Triton-X100, 0.05 mg/mL BSA). Streptavidin beads were collected on a magnetic plate and washed five times with 100 μl 50 mM ammonium bicarbonate and trypsinized with 5 μl of modified sequencing-grade trypsin (200 ng/μl; Promega) overnight in a 37 °C incubator. The samples were again placed on a magnetic plate to collect the beads and the digested sample was removed. Trypsinized samples were then dried in a Speed-Vac for one hour, and protein extracts were re-suspended in 50 μl of HPLC solvent A (2.5% acetonitrile, 0.1% formic acid) and desalted by STAGE tip.[51] On the day of analysis, the samples were reconstituted in 10 μl of HPLC solvent A. A nano-scale reverse-phase HPLC capillary column was created by packing 2.6 μm C18 spherical silica beads into a fused silica capillary (100 μm inner diameter x ~30 cm length) with a flame-drawn tip.[52] After equilibrating the column, each sample was loaded via a Famos autosampler (LC Packings) onto the column. A gradient was formed and peptides were eluted with increasing concentrations of solvent B (97.5% acetonitrile, 0.1% formic acid). Eluted peptides were subjected to electrospray ionization and then entered into an LTQ Orbitrap Velos Elite ion-trap mass spectrometer (Thermo Fisher Scientific). Peptides were detected, isolated, and fragmented to produce a tandem mass spectrum of specific fragment ions for each peptide. Peptide sequences (and hence protein identity) were determined by matching protein databases with the acquired fragmentation pattern by the software program, Sequest (Thermo Fisher Scientific).[53] All databases include a reversed version of all the sequences and the data was filtered to between 1-2% peptide false discovery rate.

Please cite this article in press as: Allard et al., A host organelle integrates stolen chloroplasts for animal photosynthesis, Cell (2025), https://doi.org/10.1016/j.cell.2025.06.003



### Electron microscopy

Electron microscopy was performed by the Harvard Medical School Electron Microscopy Core Facility according to standard protocols. Briefly, small pieces (1-2 mm cubes) of slug tissue were fixed in 2.5% glutaraldehyde and 2% paraformaldehyde in 0.1 M sodium cacodylate buffer (pH 7.4) for two hours, washed in 0.1 M cacodylate buffer, and postfixed with 1% osmium tetroxide and 1.5% potassium ferrocyanide for 1 hour. Samples were washed 2x in water, 1x in 50 mM maleate buffer pH 5.15 (MB) and incubated in 1% uranyl acetate in MB for 1 hr, followed by 1 wash in MB, 2x wash in water, and subsequent dehydration in grades of alcohol (10 min each; 50%, 70%, 90%, 100% twice). The samples were then put in propylene oxide for 1 hr and infiltrated overnight in a 1:1 mixture of propylene oxide and TAAB Epon (TAAB Laboratories Equipment Ltd). The following day the samples were embedded in TAAB Epon and polymerized at 60°C for 48 hrs. Ultrathin sections (50-80 nm) were cut on a Reichert Ultracut-S microtome, picked up on to copper grids stained with lead citrate and examined in a JEOL 1200EX Transmission electron microscope and images were recorded with an AMT 2k CCD camera.

### *In vivo* photosynthesis

Photosynthetic activity of sequestered chloroplasts in slugs was measured using pulse-amplitude modulated (PAM) fluorometry. Individual slugs were incubated at 26 °C in seawater with or without 100 μM DCMU, a photosynthesis inhibitor, under bright light. Prior to measurements, slugs were dark acclimated for 20 mins to release all photosynthetic reaction centers from light-dependent reactions that would minimize total photosynthetic potential. Maximum effective quantum yield (Fv/Fm) of photosystem II was determined by an Imaging-PAM fluorometers (Walz).

### Respirometry

Net oxygen fluxes for Elysia slugs were measured in sealed glass chambers at 25 °C using a Clark- type oxygen electrode (Unisense) that was calibrated with anoxic (bubbling with $N_2$ gas) and 100% air-saturated 0.2 μm-filtered seawater (FSW). Experimental chambers were stirred with an internal magnetic stir bar and temperature was maintained via water bath. Data were recorded using SensorTrace software (v3.4.3; Unisense).

Dark respiration and net photosynthesis were measured under 0 μmol photons $m^{-2}$ $s^{-1}$ (μE) or 500 μE, respectively, provided by an ACE Light Source with a full-spectrum halogen EKE lamp (Schott AG) calibrated with a MQ-510 full-spectrum quantum sensor (Apogee Instruments, Inc.). Briefly, an animal was acclimated to either light condition for 30 min before moving to a chamber with fresh 100% air-saturated FSW. $O_2$ fluxes were measured for 15 min in FSW, followed by a complete replacement with either 0.1% (v/v) DMSO FSW, 10 μM 5-BDBD FSW, or 100 μM DCMU FSW. $O_2$ levels were recorded for another 15 min following treatment addition.

Dark respiration and net photosynthesis were determined by manually fitting a trendline to the linear portion of the curves before and after treatment addition in order to ignore $O_2$ spikes associated with sudden slug movement (MATLAB R2022a). Trendlines were fit in a blind manner: $O_2$ curves were displayed without identifiers and a trendline fit by an independent person. Only data from the center of the curves were considered (200-800 sec). Relative dark respiration and net photosynthesis were determined by dividing the treated (DMSO, 5-BDBD, DCMU) $O_2$ flux by the untreated $O_2$ flux of the same animal. Outliers were removed using the ROUT method at 1% sensitivity and data normality and homogeneity of variance were tested using the Shapiro-Wilk normality test. Respiration data were analyzed using a matched Friedman test with Dunn's multiple comparisons test.

### Patch-clamp electrophysiology

Kleptosomes were isolated by dissecting 2-3 mm of parapodia tissue, digesting in 10 mg/mL protease type XIV in 50% seawater at 37 °C for 30min, light mechanical disruption, and filtration through a 70 μm cell strainer. 1mM vacuolin was present throughout organelle isolation. 5 mg/mL FM1-43 was then added to visualize kleptosome membranes for patch clamp experiments. To record enlarged endolysosomes, transfected cells were treated with 1μM vacuolin-1 (EMD Millipore) for 6–12hr before the patch clamp experiments. Endolysosomes were individually dissected for patch clamp experiments using a borosilicate patch pipette to cut the cell membrane and push out individual organelles which were then patch clamped with a separate pipette.

Patch-clamp recordings were carried out at room temperature using a MultiClamp 700B amplifier (Axon Instruments) and digitized using a Digidata 1550B (Axon Instruments) interface and pClamp software (Axon Instruments). Whole-cell recording data were filtered at 1kHz and sampled at 10 kHz. Membrane potentials were corrected for liquid junction potentials. Organelle currents were recorded using borosilicate glass pipettes polished to 6–7 MΩ for lysosomes and 7–12 MΩ for kleptosomes. Standard pipette/lumen solutions contained (mM): 140 NaCl, 5 K-gluconate, 3 $CaCl_2$, 20 HEPES, pH 4.6 or 7.4. Standard bath/cytoplasmic solution contained (mM): 140 K-gluconate, 5 NaCl, 0.39 $CaCl_2$, 1 EGTA ($Ca^{2+}$ buffered to 100 nM), 20 HEPES, pH 7.2. The holding potential was 0 mV and currents were measured in response to 500 ms voltage ramps from −120 to +80 mV, unless otherwise stated.

### Imaging Plastid Autofluorescence

Individual slugs were sacrificed by rapid decapitation and cut into small pieces several millimeters long and embedded in OCT, frozen, and sectioned using a cryostat (Leica CM3050S) at 18-20 μm sections and mounted on Superfrost slides (Fischer Scientific). Tissue sections were washed twice in ASW, mounted in ASW, and used within ten minutes of thawing. Spectral properties were measured by configuring a confocal microscope to excite plastids with a 405nm laser and emission intensity was measured in 50 nm bins spanning 400-700 nm light. Individual plastids were identified, segmented, and measured using the MorphoLibJ plugin's

Please cite this article in press as: Allard et al., A host organelle integrates stolen chloroplasts for animal photosynthesis, Cell (2025), https://doi.org/10.1016/j.cell.2025.06.003





segmentation tools in FIJI. The brightest autofluorescence was measured in the longest wavelength (far-red, 650-700 nm) bins, consistent with chlorophyll in functional chloroplasts, but we also observed an intensity peak in the 500-550 nm (green) bin, which corresponded to emission from a different population of plastids.

## QUANTIFICATION AND STATISTICAL ANALYSIS

For each experiment, the chosen statistical test and its result is indicated in the figure legend. Electrophysiology data were analyzed with Clampfit (Axon Instruments), while all statistical tests were performed using Prism (Graphpad). Summary data represented as mean ± SEM unless otherwise noted. N represented independent experiments using different organelles, cells, animals, as indicated for each experiment. Comparisons were considered significant if $p < 0.05$ for each indicated test. All statistical tests were selected considering the specific experiment, type of data, and anticipated distribution. Sample sizes were selected for each experiment based on convention, technical feasibility, and ethical considerations regarding animal use and availability, with a minimum of 3 replicates.

# Supplemental figures

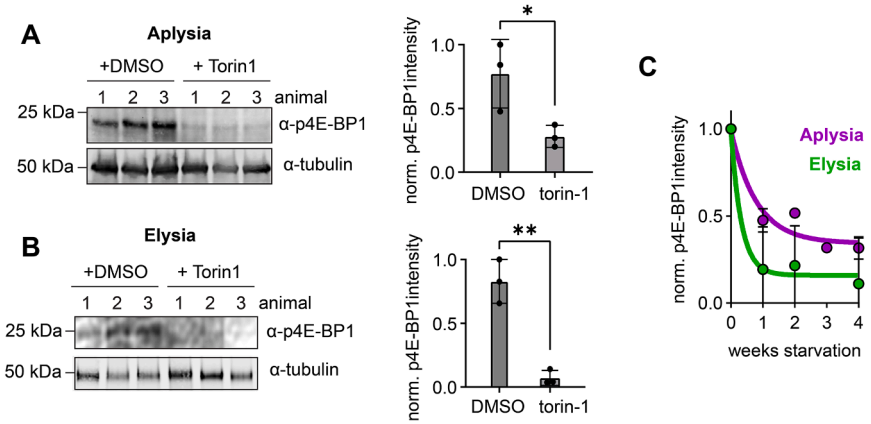
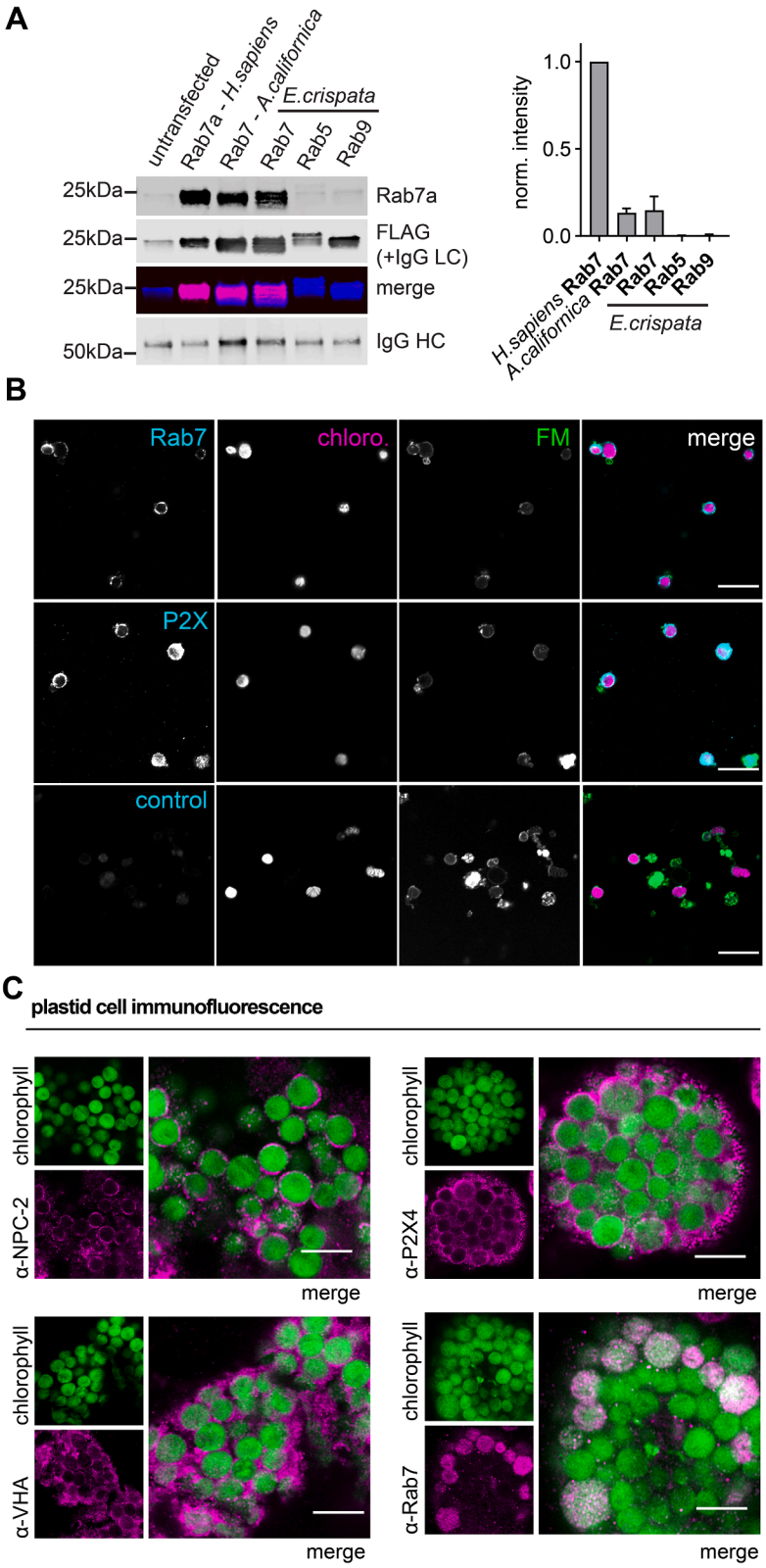



**Figure S1. Biochemical analysis of starvation, related to Figure 1**

(A) Western blots of *Aplysia* treated with 2.5 uM Torin-1 or DMSO for 24 h. Tubulin blots serve as loading controls. $n = 3$ animals per treatment. Unpaired t test, $p = 0.0392$ (*).

(B) Western blots of *Elysia* treated with 2.5 uM Torin-1 or DMSO for 24 h. Tubulin blots serve as loading controls. $n = 3$ animals per treatment. Unpaired t test, $p = 0.0020$ (**).

(C) Normalized quantification of p4EBP1 band intensities from Figure 1F. $n = 3$ replicate blots.




(legend on next page)

**Figure S2. Histology and biochemistry of kleptosomes and plastid cells, related to Figure 2**

(A) Western blots of recombinant human, *Aplysia*, and *Elysia* Rab proteins show specificity of Rab7 antibody across species. All constructs contained a FLAG tag as a control.

(B) Histology controls of dissociated kleptosomes showing a field of organelles and negative controls without primary antibodies. Scale bar, 10 μm.

(C) Endosomal and lysosomal proteins NPC2, VHA, P2X4, and Rab7 (magenta) localize to kleptosomal membranes containing chloroplasts (chlorophyll autofluorescence in green). Scale bar, 5 μm.

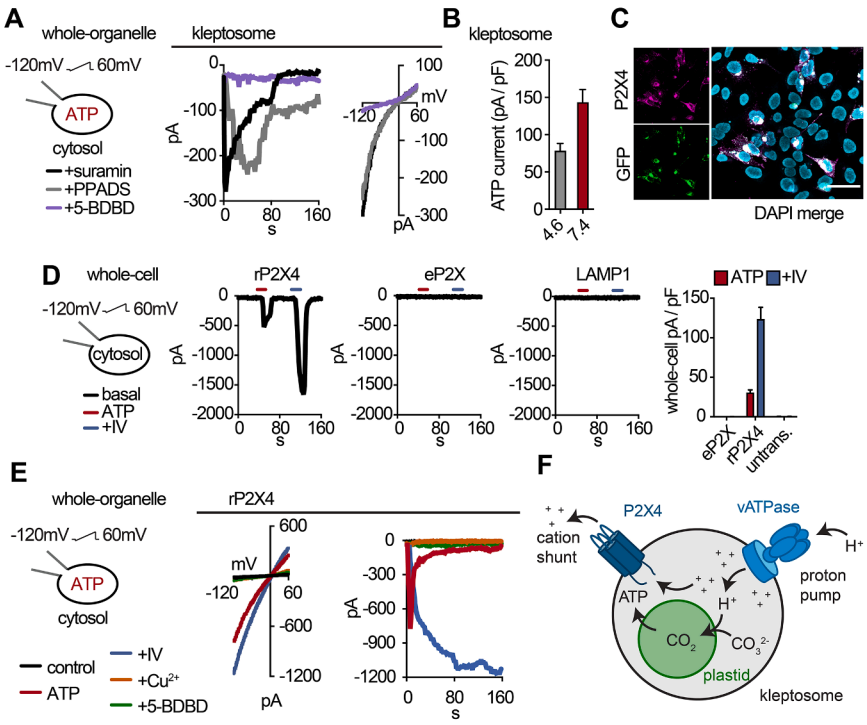



**Figure S3. Kleptosome membrane markers and electrophysiology, related to Figure 3**

(A) Kleptosome ATP-activated currents were blocked by 100 μM 5-BDBD but still measured in the presence of P2X antagonists 300 μM suramin or 300 μM PPADS.

(B) Kleptosome ATP-activated currents were reduced by acidic pH. $n = 3$, $p < 0.05$, two-tailed Student's t test.

(C) Expressed eP2X4 tagged with GFP in HEK293 stains with P2X4 antibodies used on kleptosomes from Figure 1. Scale bar, 10 μm.

(D) (Left) Whole-cell currents were recorded from HEK293 cells expressing rP2X4, which localizes to both endolysosomes and plasma membranes but not eP2X4, similar to LAMP1 controls. This suggests that functional eP2X4 localizes to only endolysosomes. (Right) Average whole-cell currents from HEK293 expressing eP2X4, rP2X, or untransfected in response to 1 mM ATP or 1 mM ATP + 5 μM ivermectin. $p < 0.001$, two-way ANOVA with post hoc Tukey test ($n = 6$).

(E) Representative whole-endolysosomal currents from rP2X4 recorded in response to voltage ramps show that native kleptosomes exhibited ATP-sensitive currents that were enhanced by ivermectin and inhibited by P2X4 blockers 500 μM $Cu^{2+}$ or 100 μM 5-BDBD. Averages are shown in Figure 3.

(F) Model of proposed cooperativity by P2X4 and the V-ATPase proton pump to support photosynthesis in kleptosomes. V-ATPase pumps protons into the kleptosome lumen, where they react with bicarbonate to produce $CO_2$ as a substrate for photosynthesis. ATP produced by photosynthesis could gate P2X4 channels, serving as a shunt for positive charge out of the lumen to facilitate the pumping of more protons into the lumen as they are consumed by photosynthesis.

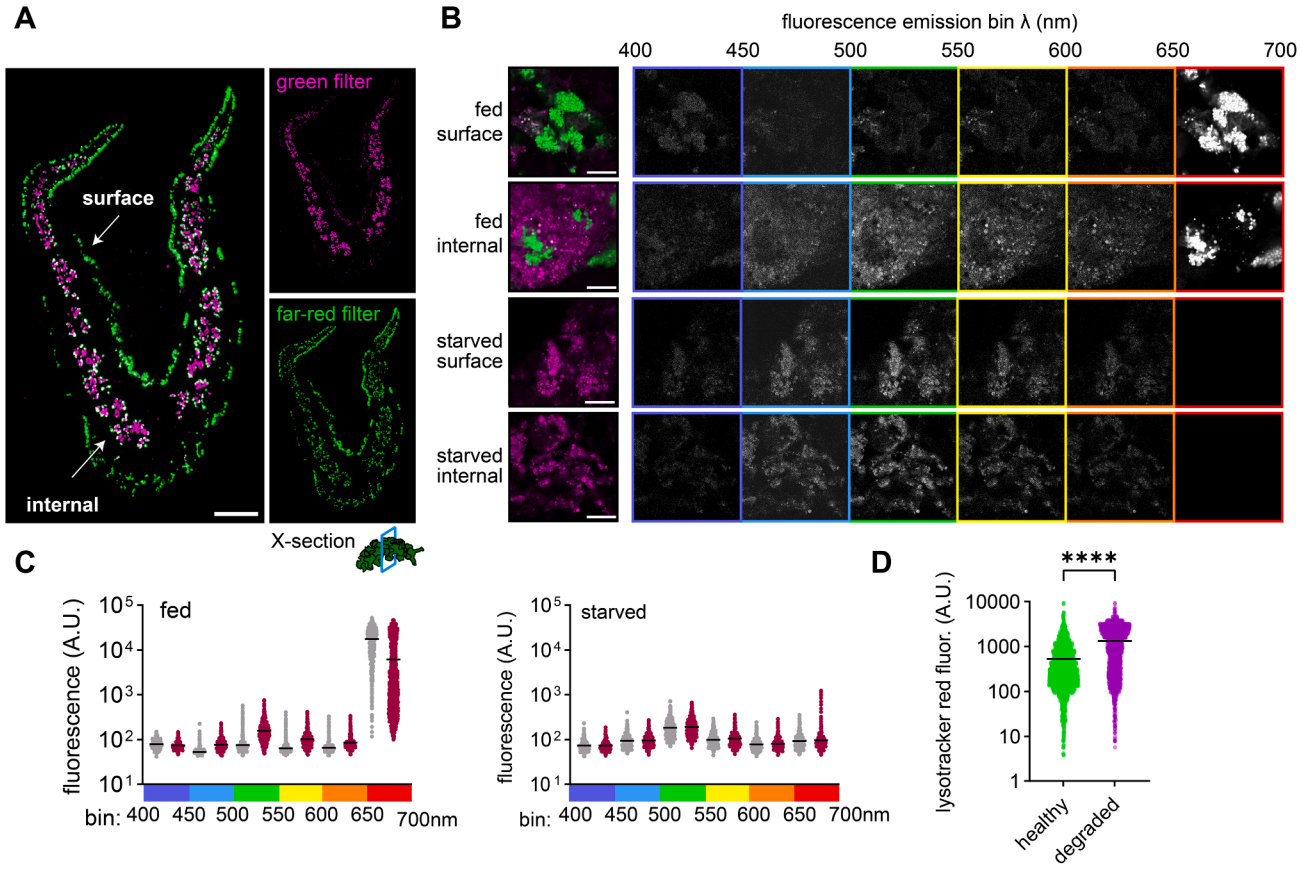



**Figure S4. Spectral properties of stolen chloroplasts, related to Figure 4**

(A) Cross section of slug shows healthy chloroplasts emitting far-red autofluorescence are enriched in near-surface plastid cells, whereas degraded and partially degraded chloroplasts are found in digestive tract lumen.

(B) Fluorescence emission of stolen chloroplasts measured in plastid cells (surface) or digestive tract (internal) in both fed and starved slugs. Healthy chloroplasts emit strongly in the far red (650–700 nm), whereas degraded chloroplasts emit primarily in green (500–550 nm).

(C) Comparison of chloroplast autofluorescence in fed and starved slugs comparing internal and surface chloroplasts.

(D) LysoTracker staining is most enriched in organelles containing degraded chloroplasts that show dim autofluorescence. Surface ROIs measure plastid cells in green, and internal ROIs measure chloroplasts in the digestive tract in magenta.

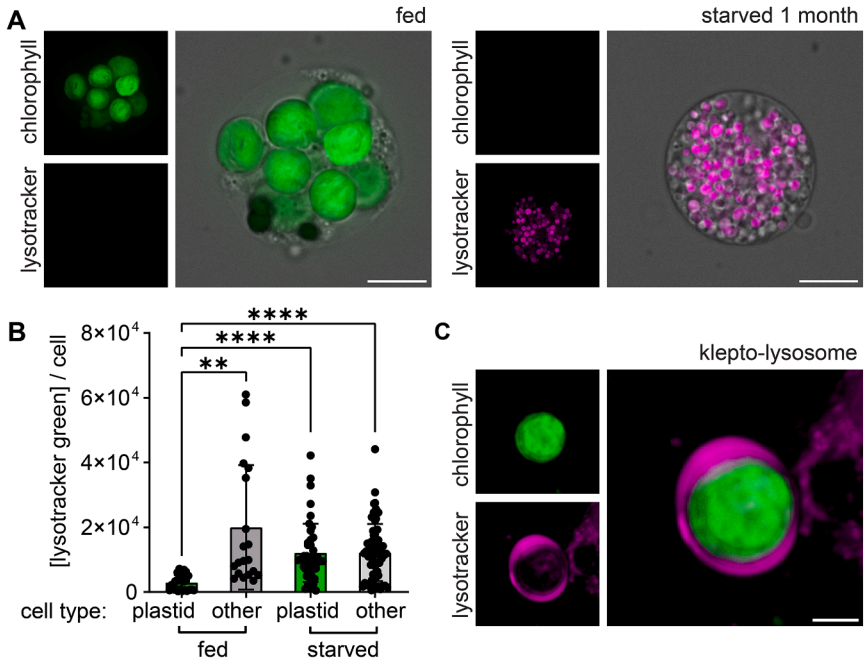



**Figure S5. Lysosome abundance in fed and starved slugs, related to Figure 4**

(A) (Left) Plastid cells isolated from fed slugs contain many kleptosomes (green) but few to no lysosomes (magenta). Cells isolated from starved slugs accumulate lysosomes and lose kleptosomes. Lysosome staining by LysoTracker green. Scale bar, 10 μm.

(B) Quantification of lysosome abundance in plastid cells vs. non-plastid cells isolated from fed and starved slugs from images as in (A). Values represent average whole-cell fluorescence intensity. $n$ = 20–60 cells per treatment sand type. Dunnett's T3 multiple comparisons test, $p_{adj}$ = 0.0024 (**) plastid cells (fed) vs. other cells (fed), <0.0001 (****) plastid cells (fed) vs. plastid cells (starved), <0.0001 (****) plastid cells (fed) vs. other cells (starved).

(C) Higher magnification image of a kleptosome that stains positive for LysoTracker green, consistent with the onset of digestion. Scale bar, 2 μm.